PHYSICAL SECTIONING IN 3D BIOLOGICAL MICROSCOPY

A Thesis

by

JYOTHI SWAROOP GUNTUPALLI

Submitted to the Office of Graduate Studies of
Texas A&M University
in partial fulfillment of the requirements for the degree of

MASTER OF SCIENCE

December 2007

Major Subject: Computer Science

PHYSICAL SECTIONING IN 3D BIOLOGICAL MICROSCOPY

A Thesis

by

JYOTHI SWAROOP GUNTUPALLI

Submitted to the Office of Graduate Studies of
Texas A&M University
in partial fulfillment of the requirements for the degree of

MASTER OF SCIENCE

Approved by:

Co-Chairs of Committee,	Yoonsuck Choe
	Bruce H. McCormick
Committee Members,	Andrew Jiang
	Jay Walton
	Marian Wiercigroch
Head of Department,	Valerie E. Taylor

December 2007

Major Subject: Computer Science

ABSTRACT

Physical Sectioning in 3D Biological Microscopy.

(December 2007)

Jyothi Swaroop Guntupalli, B.Tech, Indian Institute of Technology, Madras, India

Co–Chairs of Advisory Committee: Dr. Yoonsuck Choe
Dr. Bruce H. McCormick

Our ability to analyze the microstructure of biological tissue in three dimensions (3D) has proven invaluable in modeling its functionality, and therefore providing a better understanding of the basic mechanisms of life. Volumetric imaging of tissue at the cellular level, using serial imaging of consecutive tissue sections, provides such ability to acquire microstructure in 3D. Three-dimensional light microscopy in biology can be broadly classified as using either *optical sectioning* or *physical sectioning*. Due to the inherent limitations on the depth resolution in optical sectioning, and the recent introduction of novel techniques, physical sectioning has become the sought-out method to obtain high-resolution volumetric tissue structure data. To meet this demand with increased processing speed in 3D biological imaging, this thesis provides an engineering study and formulation of the tissue sectioning process. The knife-edge scanning microscopy (KESM), a novel physical sectioning and imaging instrument developed in the Brain Networks Laboratory at Texas A&M University, has been used for the purpose of this study. However, the modes of characterizing chatter and its measurement are equally applicable to all current variants of 3D biological microscopy using physical

sectioning.

We focus on chatter in the physical sectioning process, principally characterizing it by its geometric and optical attributes. Some important nonlinear dynamical models of chatter in the sectioning process, drawn from the metal machining literature, are introduced and compared with observed measurements of chatter in the tissue cutting process. To understand the effects of the embedding polymer on tissue sectioning, we discuss methods to characterize the polymer material and present polymer measurements. Image processing techniques are introduced as a method to abate chatter artifacts in the volumetric data that has already been obtained. Ultra-precise machining techniques, using (1) free-form nanomachining and (2) an oscillating knife, are introduced as potential ways to acquire chatter-free higher-resolution volumetric data in less time. Finally, conclusions of our study and future work conclude the thesis.

In this thesis, we conclude that to achieve ultrathin sectioning and high-resolution imaging, embedded plastic should be soft. To overcome the machining defects of soft plastics, we suggested free-form nanomachining and sectioning with an oscillating knife.

To my family and friends

ACKNOWLEDGEMENTS

First and foremost, I would like to express my deep gratitude for my research advisors, Dr. Bruce H. McCormick and Dr. Yoonsuck Choe, for their guidance and encouragement throughout my research. I would like to thank Dr. William M. Lively and Dr. Dick B. Simmons for financially supporting my graduate education. I would also like to thank David M. Mayerich and Jaerock Kwon for helping me with the KESM, Dr. Louise Abbott for various embedding samples, Dr. Gang Liang for helping me with the measurements, and Dr. Arum Han for his timely help. Finally, I thank my family and friends for their endless support. This thesis research was supported in part by National Institute of Neurological Disorders and Stroke (Award #1R01-NS54252; PI: Yoonsuck Choe).

TABLE OF CONTENTS

CHAPTER Page

CHAPTER Page

LIST OF FIGURES

Page

Page

Page

LIST OF TABLES

CHAPTER I

INTRODUCTION

A. Introduction

Our ability to analyze the microstructure of biological tissue in three dimensions has proven to be invaluable in modeling its functionality, and therefore providing a better understanding of the basic mechanisms of life. Traditionally, tissue structures are observed under a 2D microscope, which limits imaging to two-dimensional observations. Since tissues are intrinsically 3D, only limited information about their microstructure is available through this method. Volumetric imaging of tissue at the cellular level, using serial imaging of consecutive tissue sections, provides the ability to acquire its structure in 3D. This is done by using 3D microscopy.

3D biological microscopy can be broadly classified as using either *optical sectioning* or *physical sectioning*. As the names indicate, optical sectioning uses a varying focal plane to scan the image of tissues at different planes, whereas physical sectioning cuts the tissue as consecutive serial sections and images them to obtain comparable information. By first aligning and then stacking the images from consecutive planes, volumetric image data can be constructed from either optical or physical sectioning. This 3D cellular structure can further be used to reconstruct and subsequently analyze

---

This thesis follows the style and format of *IEEE Transactions on Visualization and Computer Graphics*.

structural aspects of the tissue.

B. Motivation

Each of these techniques of 3D biological microscopy, using optical or physical sectioning, has its own advantages and limitations. For example, optical sectioning restricts the maximum observable thickness of the tissue and therefore limits Z-axis resolution. These limitations stem from light scattering and diffraction-limited optics and hence are difficult to overcome. Physical sectioning, on the other hand, destroys the tissue and is in general slower than the optical sectioning. But in recent times, physical sectioning has been gaining interest in biological 3D microscopy. Introduction of novel techniques, like (1) concurrent imaging while sectioning (Knife Edge Scanning Microscopy, KESM), (2) preserving tissue sections for future analysis (Automatic Tape-Collecting Lathe Ultra-Microtomy, ATLUM) and (3) performing multiple-immunofluorescence imaging (Array Tomography), has helped physical sectioning become the sought-out method to obtain high-resolution volumetric tissue structure data. As the demands for higher resolution and increased processing speed have grown, a need has arisen for an engineering study and formulation of the tissue sectioning process.

C. Outline

This thesis addresses the following issues regarding tissue sectioning for 3D microscopy:

1. Geometric and optical characterization of the sectioning process.
2. Characterization of the embedding polymer of the tissue specimen.
3. Nonlinear dynamical modeling of the sectioning process.

4. Methods for abatement of chatter in the sectioning process.

Chapter II gives the background of 3D biological sectioning process by discussing various methods of physical sectioning currently being used. Chatter phenomenon, as it appears in the sectioning process, is introduced in Chapter III, with special emphasis on chatter in KESM. Chapter IV discusses various characterization techniques of the sectioning process, principally describing its geometric characterization and optical characterization. Chapter V discusses the measurement and analysis of KESM diamond knife vibration during sectioning. Techniques to characterize the embedding polymers and their measurement are presented in Chapter VI. Chapter VII introduces some important nonlinear dynamical models, drawn from the metal machining literature, of chatter in the sectioning process. Here models of the chatter generation in KESM sectioning process are presented and compared with observed measurements of chatter in the tissue cutting process. Image processing techniques to abate chatter artifacts are discusses in Chapter VIII. Free-form nanomachining, introduced as an ultra-precise machining technique in Chapter IX, can be adapted to the biological sectioning process. Nanomachining offers the potential to acquire chatter-free high-resolution volumetric data in less time. Chapter X discusses sectioning with the oscillating knife and how it might improve Z-axis resolution and the quality of the data. Conclusions and contributions of this thesis along with the future work are presented in Chapter XI.

CHAPTER II

BACKGROUND

A. Introduction

Volumetric imaging of tissue at the cellular level can be broadly classified as using either optical sectioning or physical sectioning. Each of these methods has its own advantages and limitations. Various microscopy techniques following these methods are discussed and compared in this chapter.

B. Optical sectioning

In optical sectioning, tissue is imaged at different depths by varying the depth of the specimen plane of the objective. In addition to the section of interest, light from out-of-focus sections contaminates the image. Computational techniques, called deconvolution, have been developed to minimize or eliminate interference from out-of-focus regions, and have been used to estimate the volumetric data set from an aligned stack of serial sectional images [1].

Physically-based techniques used for optical sectioning include differential interference contrast microscopy (DIC), confocal microscopy, and multi-photon microscopy. The ability to image live biological tissue is a major advantage of these techniques. Although images obtained by these techniques are called “optical sections”, they differ from true sections in that their vertical boundaries are not sharply defined. The 3D point spread function (PSF) of any optical system is elongated in the vertical

direction, so any point in the tissue has its intensity spread across multiple sections [1]. Hence, section thickness is ill-defined. A commonly-used measurement for optical sectioning, ,analogous to section thickness, is Full Width at Half-Maximum (FWHM), the width at half-amplitude of the curve that describes the relative intensity of points at different distances from the midpoint of the section. FWHM for confocal microscopy is typically comparable to 600nm [1]. To obtain the highest depth resolution possible, adjacent optical sections must be placed at increments of roughly half the FWHM of the vertical PSF. This limits the section thickness to 300nm in this technique. Due to the limitations optical sectioning places upon the thickness of the tissue and Z-axis resolution, physical sectioning is gaining interest in biological 3D microscopy.

C. Physical sectioning

Imaging methods based on physical sectioning use four processing steps: staining, embedding, sectioning, and imaging of the tissue. Tissue of interest is sectioned into slices of desired thickness, typically using an ultramicrotome, based on the choice of staining technology and required axial resolution. Images of successive sections are aligned and stacked in registration to obtain a volumetric data set. The tissue staining step can precede the sectioning step using an en bloc staining technique, wherein the entire specimen block is stained a priori. These four steps are more or less independent of each other, which makes this method slower than optical sectioning. In fact, this characteristic allows the use of multiple imaging techniques on the same tissue section, irrespective of its sectioning process. Unlike in optical sectioning, tissue is destroyed by the physical sectioning process and therefore the method does not allow imaging of live tissue. The speed of this method is limited by the time it takes for sectioning, staining, and imaging.

With the advent of high precision machining tools and automation of the cutting process, physical sectioning is emerging as a preferred choice for volumetric imaging of biological tissues. Knife Edge Scanning Microscope (KESM), Automatic Tape-Collecting Lathe-Ultramicrotome (ATLUM), Array tomography, Serial block-face scanning electron microscopy (SBF-SEM), and Serial section transmission electron microscopy are some of the methods using physical sectioning (Table 1). These are discussed in detail in subsequent sections.

D. Knife-Edge Scanning Microscope (KESM)

The Knife-Edge Scanning Microscope (KESM) (Fig. 2A), invented by Bruce H. McCormick and developed by associates in the Brain Networks Laboratory at Texas A&M University, affords a novel technique in light microscopy for cellular-level volumetric dataset acquisition. It has been demonstrated that it is possible to create cellular datasets of 1cm3 in approximately 3 weeks [2]. The specimen is first en bloc stained and then sectioned. For sectioning, a vertical stack of three mechanical stages move the workpiece, a block of polymer-embedded stained tissue, against a wedge–shaped stationary diamond knife. Sectioning and imaging are concurrent, and inter-sectional registration is maintained by line scanning the tissue section as it rolls over the tip of the top facet of the diamond knife (Fig. 1A). Typically each section is 15mm long and 0.5μm thick. Scanned images of successive sections are then stacked to obtain the volumetric data set. No further registration of the successive images is required. Tissue structure of interest is reconstructed using this 3D data (Fig. 1B).

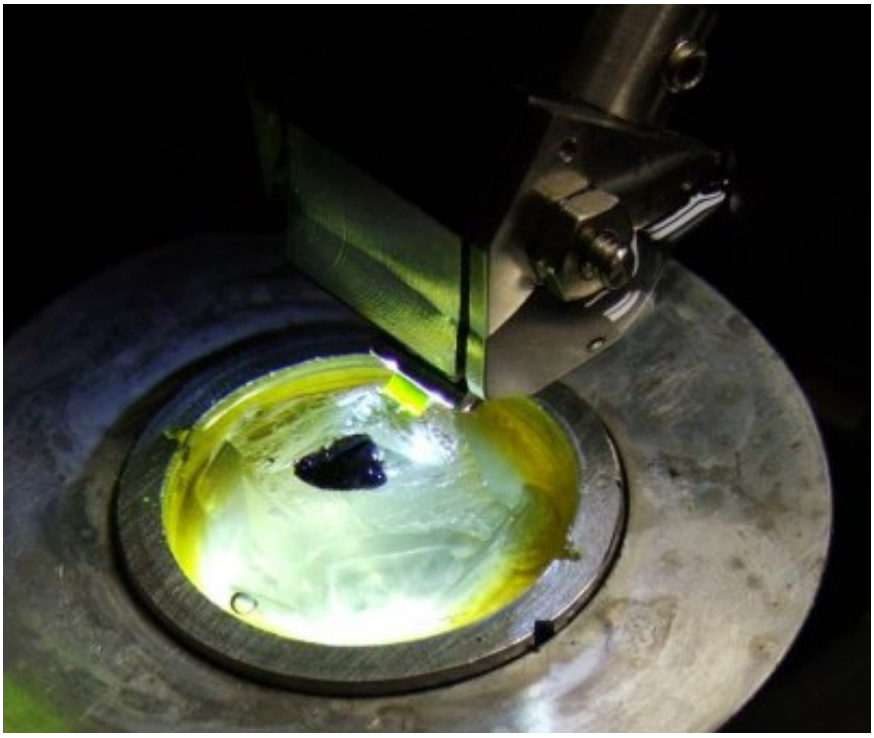

A

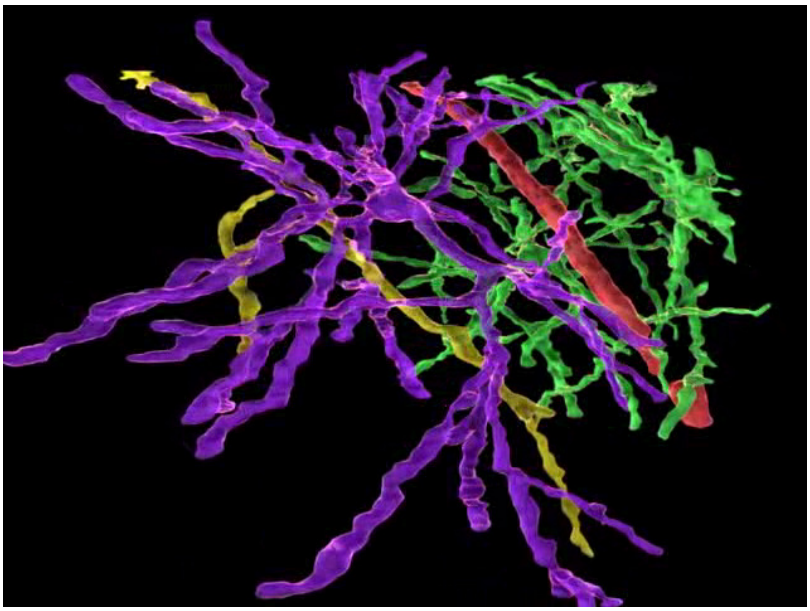

B

Fig. 1. A. Close up view of the diamond knife and the embedded tissue block in KESM, B. Neurons reconstructed from KESM data [2].

E. Automatic Tape-Collecting Lathe-Ultramicrotome (ATLUM)

The Automatic Tape-Collecting Lathe-Ultramicrotome (Fig. 3B), developed by Kenneth Hayworth at University of Southern California, is intended to automate the process of sectioning tissue volumes at ultra-thin section thickness. It uses a lathe mechanism to produce a continuous ribbon of tissue by sectioning an extremely thin strip off the surface of a cylindrical block containing a multitude of embedded tissue samples. This design has inherent advantage of abating mechanical vibration as the knife never disengages from the tissue block. The sectioned tissue is collected as a ribbon sandwiched between a pair of supporting tapes. Current section thickness has reached 45nm and the speed of sectioning 0.03mm/s [3]. Though the main intention of this project is to provide sections for transmission electron microscopy, the prototype is built for light microscopy.

F. Array tomography

Array tomography (Fig. 2C), recently invented by Stephen J. Smith and Kristina Micheva in the Department of Molecular and Cellular Physiology at Stanford School of Medicine, is a novel technique for volumetric imaging and analysis of tissues in 3D. It employs the technique of imaging an array of a large number of serial ultra-thin (50-200nm) immuno-fluorescent-stained specimen sections. A hydrophilic acrylic resin is used for embedding the tissue [4]. The embedded tissue is sectioned using a diamond-knife ultramicrotome to produce continuous ribbons of serial sections, which are then bonded in a parallel array to the surface of a glass slide. Labeled antibodies or other reagents are used to stain this 2D array of sections. The array of stained sections is then imaged using optical fluorescence or catholuminescence induced by scanning electron microscopy [4]. 3D reconstruction is achieved by alignment and collation of individual

2D section images into volumetric stacks. Antibodies can be stripped off the section quickly and thoroughly, as they are stained due to rapid diffusion through the ultra-thin sections. This allows for multiplexing very large number of immuno-stains through repeated cycles of stripping, staining, and imaging an individual array slide. Array tomography also has other advantages including high volumetric resolution (unlike the poor Z-axis resolution of optical sectioning), specimen conservation, quantitative reliability, detection sensitivity, scalable volume field of view, and direct applicability to human tissues.

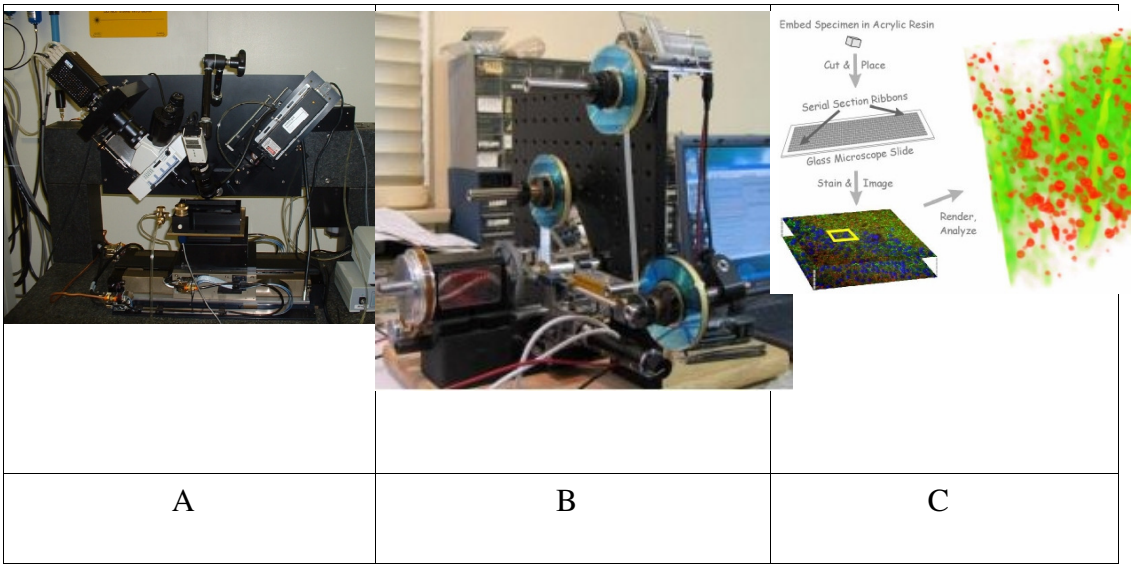

A	B	C

Fig. 2. A. KESM [2], B. ATLUM [3], and C. Array tomography [4].

G. Serial block-face SEM

Serial block-face scanning electron microscopy, developed by Winfried Denk and Heinz Horstmann at Max Plank Institute of Medical Research, Heidelberg, combines the techniques of block-face imaging (which is traditionally used for light-microscopy of gross anatomy) and scanning electron microscopy. Though Leighton introduced this technique in 1981, he was not able to image the sectioned block face at adequate contrast

because of charge build-up. Denk and Horstmann used electron backscattering detection and low-vacuum operation, to obtain high-contrast images from the cut block face [5]. Sectioning is performed within the vacuum system of the SEM [5]. Imaging the sectioned block face removes the difficulty of aligning the images of sections, as required for 3D reconstruction. Ribbons of the fragile sections are discarded, allowing for automation of volumetric data set acquisition.

H. Serial section TEM

Transmission electron microscopy requires ultra-thin sectioning of polymer-embedded tissue. En bloc staining of the tissue with heavy element stains is used. Since this method is preferred for its high resolution imaging, utmost care is taken to achieve uniform section thickness along a fold-free ribbon. Harris et al. [6] have developed a procedure to achieve long ultra-thin uniform fold-free ribbon. Ribbons obtained from the sectioning process are then imaged using a transmission electron microscope. Tissue is then reconstructed from these TEM images in 3D using software tools. Achieving a section thickness of about 50nm helps in identifying substructures such as synaptic vesicles (~35nm) and narrow axonal or astroglial processes (~50nm) [6].

Table 1 gives a comparison of microscopy techniques, described above, that use physical sectioning for 3D imaging. Parameters for the microscopy include type of microscopy (LM/EM), typical section thickness, and speed of sectioning.

Table 1. Comparison of 3D microscopy techniques using physical sectioning.

S. No.	Name	Light Microscopy (LM)	Electron Microscopy (EM)	Thickness of imaging section (nm)	Speed (mm/s)
1.	KESM	Yes	No	~500	21(maximum possible); 17(10X objective); 4.2(40X objective)
2.	ATLUM	Yes	Yes	~45	0.03
3.	Array Tomography	Yes	Yes	50-100	NA
4.	Serial Block-Face SEM	No	Yes	30-50	NA
5.	Serial Section TEM	No	Yes	40-60	NA

I. Summary

Biological 3D microscopy provides volumetric data sets of cellular structure, and can be broadly classified as either using optical sectioning or physical sectioning. In this chapter the various microscopy methods using physical sectioning were described in detail, and their basic advantages and disadvantages were summarized. Any method using physical sectioning potentially suffers from the undesired vibrations in the sectioning process called chatter. Chapter III introduces chatter in the physical sectioning process, with particular emphasis on chatter phenomena in KESM.

CHAPTER III

CHATTER IN THE SECTIONING PROCESS

A. Introduction

Of all machining techniques, metal cutting, in which material is removed from the metal workpiece using a cutting tool, is the most widely used. Machining involves relative motion between the workpiece and the cutting tool. This relative motion can give rise to many forms of undesired vibrations during the cutting process, of which mechanical chatter is the most frequently occurring and is difficult to abate. Chatter can be distinguished from other types of vibrations owing to the fact that it is a self-sustaining process and can continue unless quenched. In machining processes like milling and cutting, the effects of chatter are visible as lines or grooves on surface of the workpiece. Fig. 3 shows chatter artifacts left on a metal surface during milling [7]. These lines are usually repeated at regular intervals, based on the frequency of knife/machine vibration and the cutting speed.

Unlike from metals, plastic parts have traditionally been produced by molding processes. Although molding is fast and flexible, appropriate molds must first be machined from titanum or like metal. Therefore for manufacturing high precision plastic parts, such as contact lenses and similar parts for the photonics industry, machining is still used [8]. Direct machining of plastics also suffers from undesired vibration in the cutting tool or the workpiece during the process. Since this process is also used to manufacture

high-precision parts [9], it is of high importance to abate any such vibration. Similar considerations apply directly to biological sectioning as commonly tissues are embedded in a polymer before sectioning. The material properties of the embedding polymer limits machining of biological tissues. With an emerging demand for faster volumetric data acquisition and higher resolution, the drastic effects of chatter in both sectioning and imaging in the tissue sectioning process has become increasingly important.

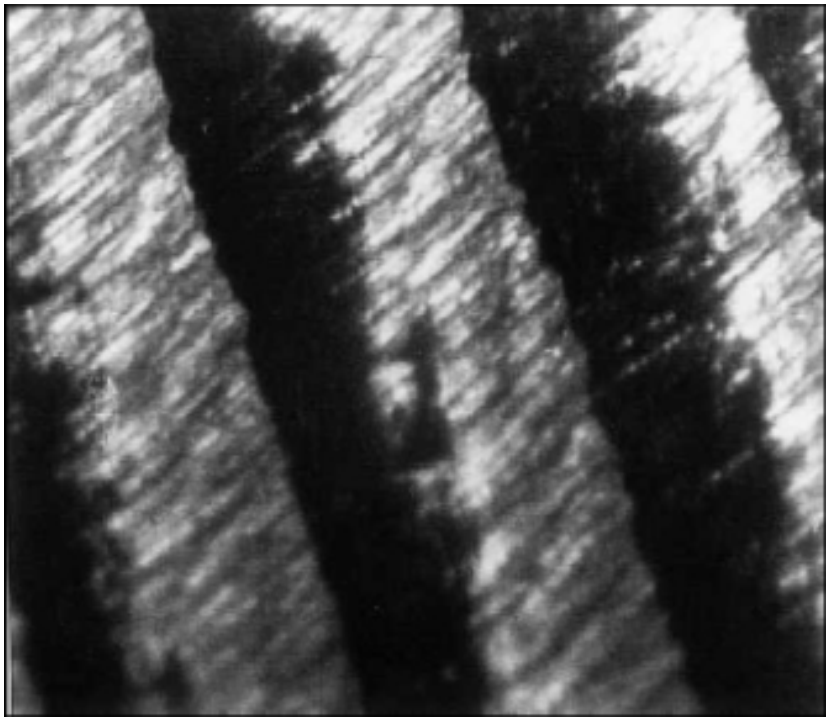

Fig. 3. Chatter (seen as alternating bands) as it appears in milling on the surface of the chip [7].

B. Types of chatter

Chatter has been classified into four types based on the source of vibration: frictional, regenerative, mode-coupling, and thermo-mechanical [7]. *Frictional chatter* gets its excitation energy from the friction force either between the workpiece and the tool

flank, or between the section (chip) and the rake surface, or both. *Regenerative chatter*, as the name indicates, regenerates from the previous cut. Since serial sectioning involves repeated cutting of the workpiece top surface, this type of chatter is the most common form of undesired self-induced vibration. Variation in cutting forces is induced when the tool cuts the uneven surface from the previous cut. This variation in force leads to vibration of the cutting tool and therefore to an uneven (wavy) surface. In this way the chatter process feeds upon itself. When the vibration in cutting force direction induces vibration in thrust force direction or vice versa, it is called *mode-coupling* chatter, which means the undesired vibrations are in two directions. Friction between the clearance and the workpiece feeds this kind of chatter. Since cutting involves plastic deformation of workpiece material, changes in strain-rate and temperature affect the process. When these changes result in chatter, it is called *thermo-mechanical chatter*.

C. Effects of chatter on physical sectioning for 3D microscopy

Chatter during sectioning leaves artifacts in image data. In case of KESM, imaging is performed simultaneously with sectioning and hence this undesired vibration shows up in the image as alternating streaks of bright and dark bands. Even in other techniques, like array tomography, where the imaging is done after the sectioning process, the image can still show alternating bright and dark patches if the tissue is illuminated from the back. These chatter artifacts make the reconstruction process both difficult and often inaccurate, as the reconstruction program can mistake these artifacts for real tissue features.

In practice, the cutting speed and/or the depth of cut are often changed in order to

abate chatter during the sectioning process. Hence chatter limits sectioning speed and subsequently the speed of volumetric data acquisition. Other means of circumventing chatter is to limit the thinness of the cut. However, thicker sectioning means lower Z-axis resolution. Chatter therefore also limits the Z-axis resolution of 3D microscopy, contradicting a principal advantage of physical sectioning – higher Z-axis resolution.

D. Chatter in the KESM sectioning process

Serial sectioning in KESM can be approximated by an *orthogonal cutting process*. A diamond knife acts as the *cutting tool* and the tissue, embedded inside a plastic (Araldite or Epoxy) block, is the *workpiece*. The diamond knife is fixed to a granite bridge, which in turn is bolted to a granite slab that also supports the three-axis linear stage. The slab is heavy and helps stabilize the system from external (e.g., room) vibration.

The workpiece, a plastic block with embedded tissue, is molded in to a keyed ring, which is then mounted inside a *specimen tank*. The key prevents the block from rotating while undergoing sectioning. This ring is held in place firmly by a set screw. As shown in Fig. 4, the entire assembly, including the tank, sits on the stage assembly of the KESM. (The diamond knife can also be translated at 45 degrees to the horizontal, so that the specimen (workpiece) can be inserted into the specimen tank atop the stage assembly.) The custom-designed stage assembly has three separate mechanical linear stages, which give the mounted specimen tank three degrees of freedom. To section the embedded tissue, the stage moves in the cutting direction against the stationary diamond knife, planing a thin section from the block. The stage then lowers, retracts back to its original

position on the X-axis, and then is incremented to the height of the new cut. This process is repeated to serially section and concurrently image the tissue. During each sectioning stroke, when the workpiece first comes in contact with the diamond knife, it hits the knife – resulting in an impact that initiates vibration in the tool. This induced vibration, unless dampened, results in an uneven cut and leaves a wavy surface on the block. Subsequent sections cut from the block retain a phase-shifted variant of this wavy surface. This process continues forever feeding upon itself unless quenched. This type of chatter is classified as *regenerative chatter.*

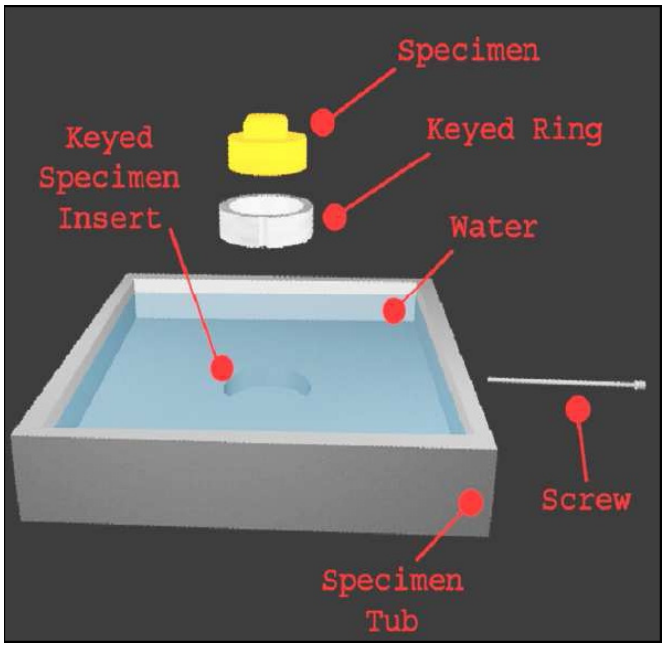

Fig. 4. Specimen assembly [2].

Optical evidence of these mechanical vibrations during the sectioning process comes from volumetric data obtained by KESM. The imaging system of the prototype KESM consists of a Nikon microscope objective and Dalsa line scan cameras to capture the image. Tissue is imaged under water to improve spatial resolution. Imaging in the

KESM uses either a 10X objective for survey studies, or a 40X objective for the higher magnification required to trace neurons and processes. Imaging at this higher magnification means even smaller vibrations in the knife can leave observable artifacts in the imaging data. Also, chatter is highly dependent upon the cutting speed and adjusting the speed of cutting changes the spatial frequency of these artifacts in the image. High-speed sectioning in the prototype KESM can reach a maximum of 21mm/s (currently limited by the line rate of the current line-scan camera) [2]. Fig. 5 shows a typical KESM image exhibiting chatter, which appears as dark horizontal streaks occurring at regular intervals along the Y-axis. Fig. 6 shows the coordinates.

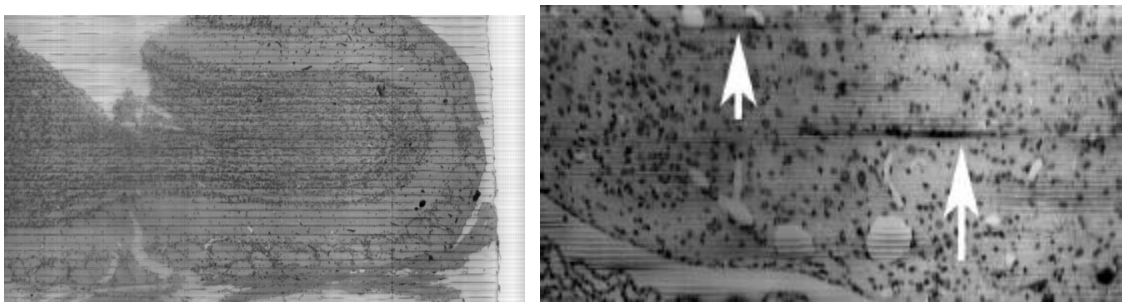

Fig. 5. KESM tissue sections showing chatter. (Left) Chatter artifacts occurring continuously in the image data. (Right) Chatter artifacts occurring as irregular streaks in the image data [10].

Knife chatter gives rise to non-uniform section thickness, which in turn appears as alternating dark and bright patches in the scanned image. Other effects, such as distortions of the embedding polymer, – even for a non-vibrating knife – can result in the similar image distortions. This stresses the need for a direct comparison of optical and geometric characterization of the chatter phenomena (see Chapter IV).

David Mayerich, doctoral candidate in Brain Networks Laboratory (BNL) at

Texas A&M University, observed that the dark streaks due to chatter in the image are aligned across successive sections with slow continuous shifts of phase. Fig. 6 shows a vertical slice of volumetric data of tissue obtained by KESM along the X-Z plane (X-axis is along the cutting direction and Z-axis is along the vertical, or depth direction). Each row represents one section (e.g. Fig. 5) viewed from the side. A surprising fact is that successive sections were cut at random velocities, varying as much as 2 to 1.

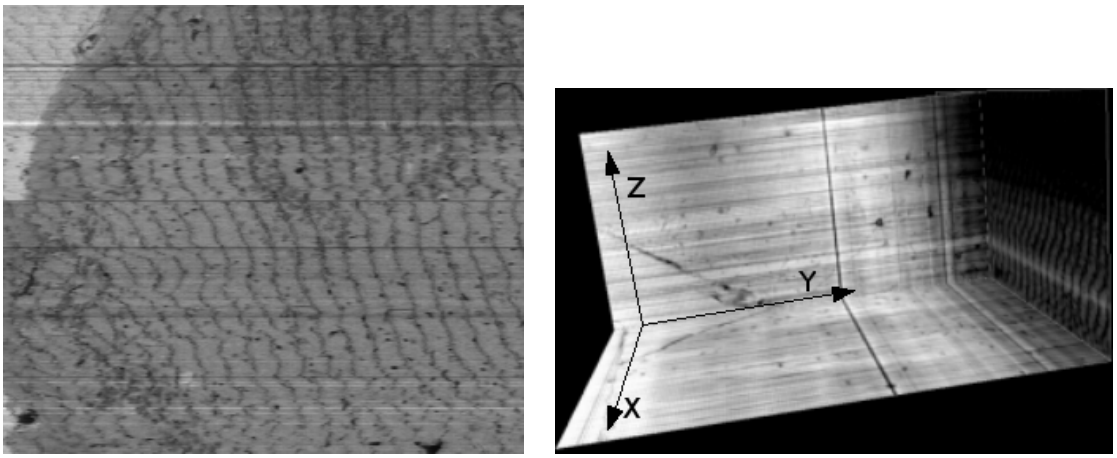

Fig. 6. (Left) Slice of volumetric image data of tissue along X-Z plane showing the alignment of chatter across successive sections. (Right) 3D view of image data showing the axes: X-cutting direction, Y-knife-edge direction, and Z-vertical direction.

Volumetric image data of tissue sectioned at relatively high speeds enabled the observation of this previously unobserved phenomenon. This observation, which apparently largely rests on the embedding polymer of the tissue, can potentially be used to abate chatter phenomenon (see free-form nanomachining, Chapter IX). Also, this observation reveals smooth transition of chatter artifacts in volumetric data, which indicates the possibility of using image processing methods to remove these artifacts (see Chapter VIII).

E. Summary

Chatter is an undesired mechanical vibration creeping into the sectioning process. It has been well studied in metal cutting, where it is considered to be a nonlinear dynamical phenomenon, but little studied in biological tissue sectioning. Chatter in biological sectioning affects the quality of reconstruction and limits Z-axis (depth) resolution and speed of sectioning. As the demand increases for faster volumetric cellular data acquisition at ever-increasing spatial resolution, chatter in the sectioning process can be expected to play an ever more important role. The next chapter discusses techniques to characterize the sectioning processes.

CHAPTER IV

CHARACTERIZATION OF PHYSICAL SECTIONING

A. Introduction

Sectioning repeatedly shapes the workpiece by using mechanical forces to shear the workpiece with the cutting tool. This basis of sectioning gives the process certain acoustic, vibrational, geometric, and optical characteristics described below.

Machining is inherently a loud process. Sound is produced during machining as atomic bonds are broken during shearing. Also, the workpiece material resists the cutting force applied by the tool, resulting in a dynamical equilibrium. If the workpiece material resistance is not uniform, then instability can creep in as vibrations in this dynamical system. These vibrations contribute to the sound of machining and are also reflected as variations in section thickness and as serrated workpiece surfaces. In the KESM, from which the data of this thesis was drawn, these instabilities also appear in the imaging data as optical artifacts (previously discussed in Chapter III.)

B. Characteristics of chatter in the sectioning process

Chatter is a form of undesired mechanical vibration that generates an audible buzz during cutting. Also, as stated earlier, chatter leaves its mark on the chip in the form of variation in section thickness. During imaging, this results in variation of brightness as the light is projected from the knife through the chip to reach the camera objective.

Chatter leaves a variation in brightness that appears as alternating dark and bright streaks in the image, based on the thickness of the chip. These two characteristics of chatter: *chatter frequency* and *chip thickness variation*, can therefore be used to quantify chatter. Based on these two characteristics, different techniques of quantifying the sectioning process in general and measuring chatter in particular, are discussed below.

C. Sound of chatter

Chatter during machining can be picked up as an unique buzzing sound, which can be easily differentiated from the background sound of machining. Recording this sound using a microphone, and its subsequent analysis gives a measure of chatter. In quantifying chatter using sound, the cutting process without chatter is recorded initially and used as the baseline, as sectioning produces some sound even without chatter. The frequency spectrum of chatter can be obtained using the Fast Fourier Transform on the recorded sound data. Chatter appears in this spectrum as unusually high amplitude vibration at certain frequencies. These can easily be distinguished from the frequency spectrum of the sound without chatter. Though this measurement does not give accurate quantification of chatter, it can be used in real-time monitoring of cutting processes and also in the active abatement of chatter. A major disadvantage of this kind of chatter measurement is the possible interference from the ambient noise.

D. Geometric characterization

Chip thickness variation and workpiece surface profile can be categorized as geometric characterizations of the sectioning process. The sectioning process is considered ideal, with no external disturbance, if the resulting chip is of uniform

thickness. This rarely happens in real-world sectioning due to undesired vibrations stemming from the variation in material properties and amplification of small cutting disturbances. Hence chip thickness profiles give a good indication of the quality of the sectioning process. Also, they are easy to measure using a multitude of commercially available instruments like profilometers and atomic force microscopes (AFM).

Fig. 7. Dektak 3 profilometer [11].

For example, KESM specimens are predominantly sectioned at a thickness of 0.5μm. An ideal section should be of uniform thickness and its profile a straight line along any line across its surface. But due to chatter and other effects, the thickness of the cut tissue section varies. Surface profile measurement of this tissue section, using a profilometer, thus gives the variation in section thickness.

E. Profilometer

A profilometer (Fig. 7) is an instrument that can be used to measure the profile of any surface along a straight line. It measures the height of the surface of any specimen by

dragging a diamond stylus attached to the free end of a cantilever. This cantilever is coupled to a linear variable differential transducer (LVDT), which converts the change in the height of the stylus into an electrical signal. The stylus tip is in continuous contact with the surface and its movement is reflected as the change in position of the core of the cantilever coupled to the LVDT. The Dektak 3 profilometer at the Material Characterization Facility at Texas A&M University (TAMU) was used to measure the profile of the section from KESM. The profilometer can measure vertical features ranging in height from 10 to 65,000nm [11]. Fig. 8 shows the profile of a chip measured using a Dektak 3 profilometer. It is evident from Fig. 8, and direct observation through a microscope during measurements, that profiling soft specimens like embedded tissues give rise to problems such as dragging and compression of the tissue surface. Also, the radius of the diamond stylus of this profilometer is 12.5µm, which means that the spatial resolution of measurement is at most 12.5µm, where in contrast each image pixel has a resolution of 0.3-0.6um (X and Y) and 0.5-2um (Z).

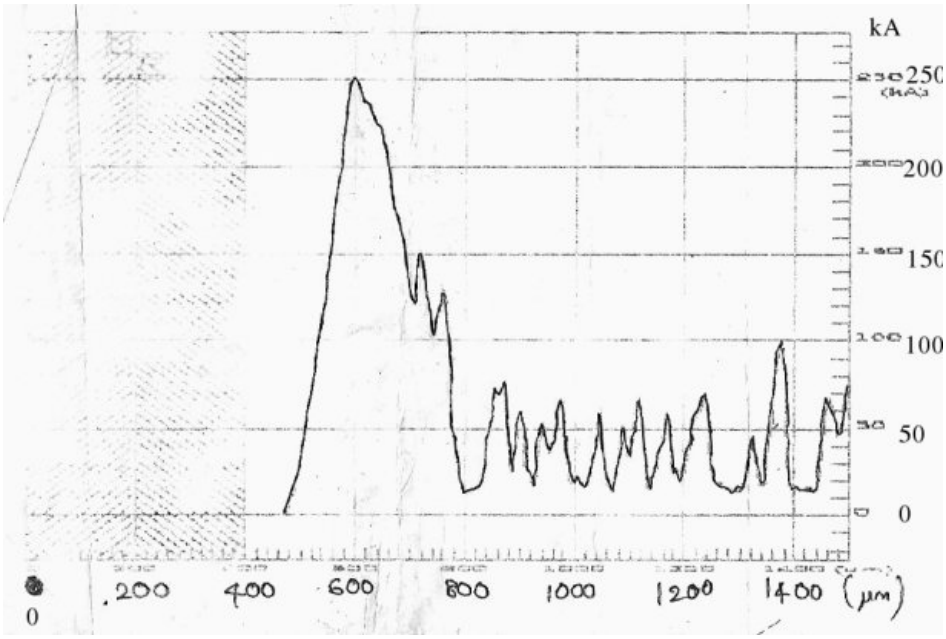

Fig. 8. Profile of a tissue section from KESM measured using the Dektak 3 profilometer. The X-axis is the scanned distance along the sample (in micrometers) and the Y-axis is the height at each sample point (in kAngstroms). Notice the peak at the beginning due to dragging of the softer tissue by the diamond stylus.

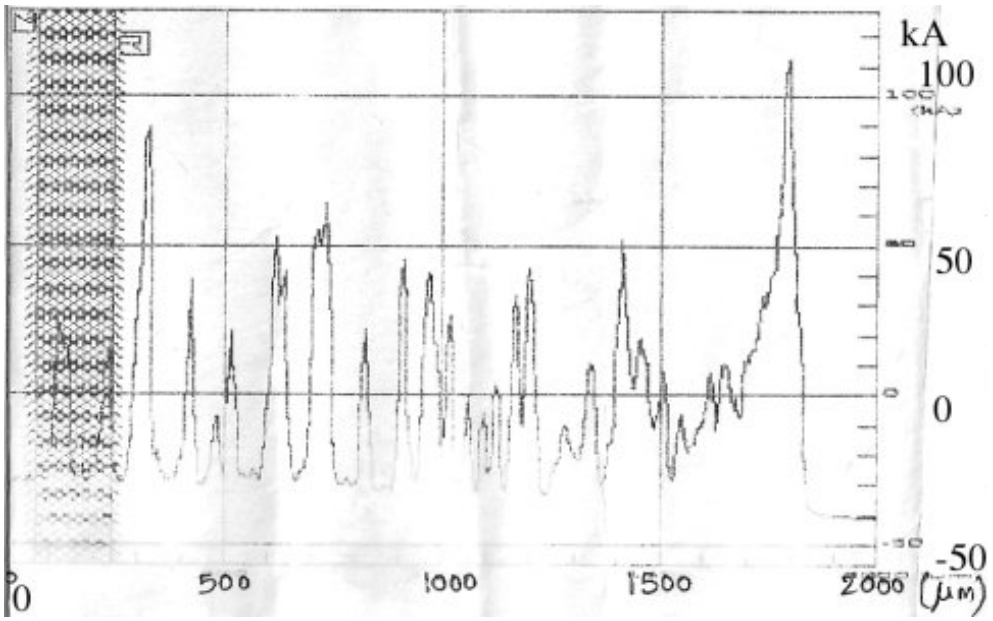

Fig. 9. Profile of a tissue section from KESM measured using Dektak 3 profilometer. The X-axis is the scanned distance along the sample (in micrometers) and the Y-axis is the height at each sample point (in kA).

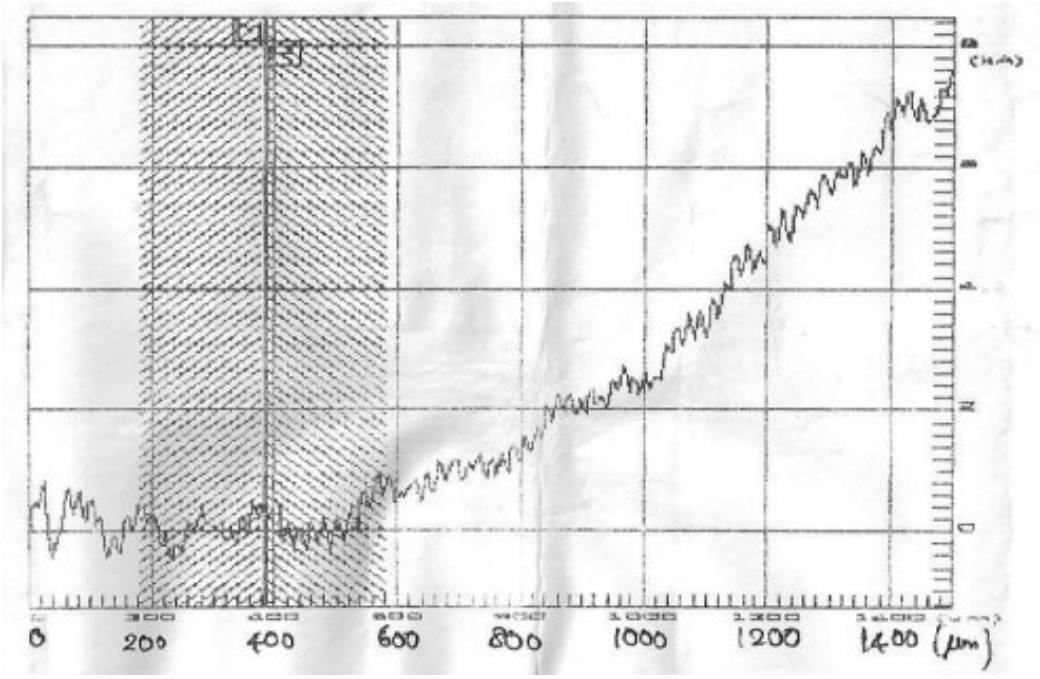

Fig. 10. Profile of a tissues section from KESM measured using Dektak 3 profilometer. The X-axis is the scanned distance along the sample (in micrometers) and the Y-axis is the height at each sample point (in kA).

Profiles of the tissue section measured at different locations using the Dektak3 profilometer are shown in Figs. 8, 9, and 10. It can be seen from the data that the variation in profile is in the order of hundreds of nanometers (1kA=100nm). Fig. 8 also shows that the tissue section, being soft, is dragged by the stylus, resulting in a pullback. Moreover, since the stylus is dragged on the measured section, tissue under the tip is under constant force to maintain contact and hence is compressed -- inducing an error in measurement.

F. Atomic force microscope

To overcome the limitations imposed by profilometers such as dragging, compression of the chip, and resolution, an atomic force microscope (AFM) was used for surface profiling the tissue section. Atomic force microscopy is a scanning probe microscope method invented by Binnig, Quate, and Gerber in 1986 [12]. Due to its

resolution in the order of nanometers, it is used extensively to image, measure, and manipulate matter at the nano-scale. Basic working principle of the AFM is shown in Fig. 11.

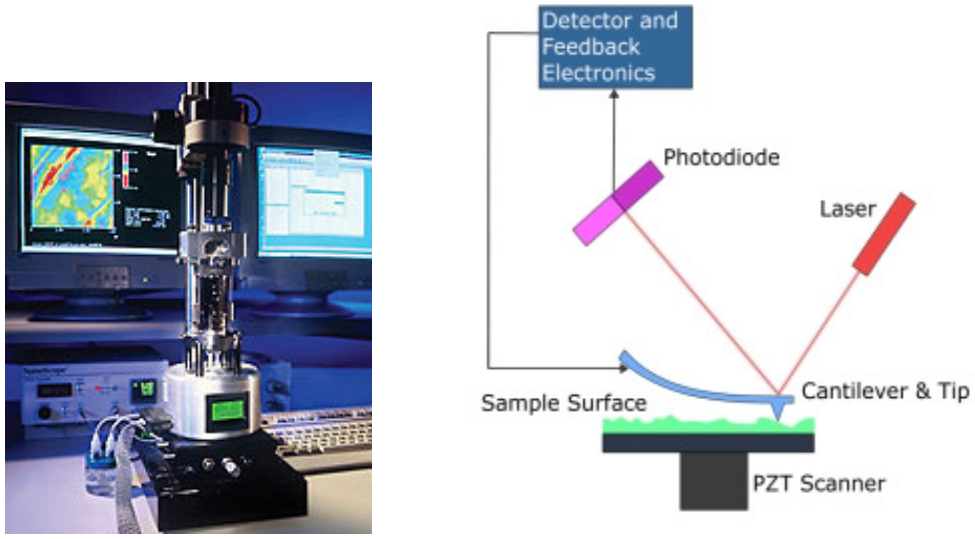

Fig. 11. Atomic force microscope [12] (left) and its schematic showing the working principle (right)

The Material Characterization Facility at Texas A&M University houses an AFM (Veeco MultiMode AFM, the highest-resolution scanning probe microscope ever manufactured [13]). The instrument allows a scan range of up to 120µm on the X–Y axes, and a Z-axis range of up to 6µm. The tapping mode of the AFM, a patented technique, allows imaging of samples that are soft. In the tapping mode, the probe is vibrated vertically by a piezoelectric oscillator to hit the surface at a regular time interval while the probe moves horizontally on the surface, touching the specimen surface only at these regular intervals.

By lightly tapping the stylus tip on the surface during scanning, lateral, shear forces are eliminated, improving image quality. Since our embedded tissues are soft, we used the tapping mode of operation. For our measurement, we used three ranges of

scanning areas: 2µmx2µm, 10µmx10µm, and 50µmx50µm to locate the appropriate scan area to recognize the chatter artifacts. For each scan range, the tip makes 512 readings in the X and Y axes, giving a 512x512 matrix of height data in nanometer resolution. Fig. 12 shows the surface profile of the chip at three different scan area ranges mentioned above.

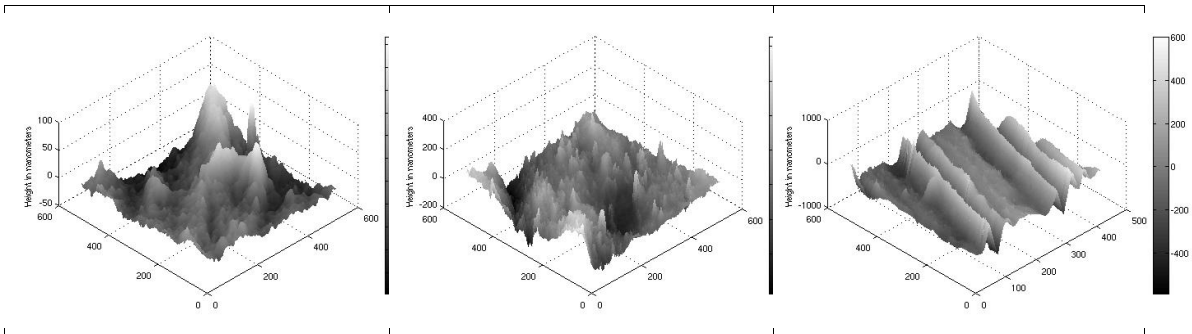

2µmx2µm	10µmx10µm	50µmx50µm

Fig. 12. Surface profile of a section from KESM measured in AFM at three different scan area ranges. The X-Y plane is the plane of the tissue section and Z-axis represents the height at each scanned point in nanometers. For any given scan area, AFM samples the height at 512x512 points on the section. So, for each scan area, x and y axes represent the index of sampling points.

It is evident from Fig. 12 that the pattern of chatter appears at the 50µmx50µm scan range. It is also observable that the variation in thickness has multiple frequencies (multi-modal). Fig. 13 shows the profile along the chatter lines. An interesting observation is that the profile of the tissue section varies as much as 500nm in both directions from the mean. This is a significant variation for a chip of 2µm thickness. Using basic trigonometry, we can calculate the distance between two successive lowest points in the tissue section to be 21.27µm. This gives the spatial frequency of chatter of ~47cycles /mm.

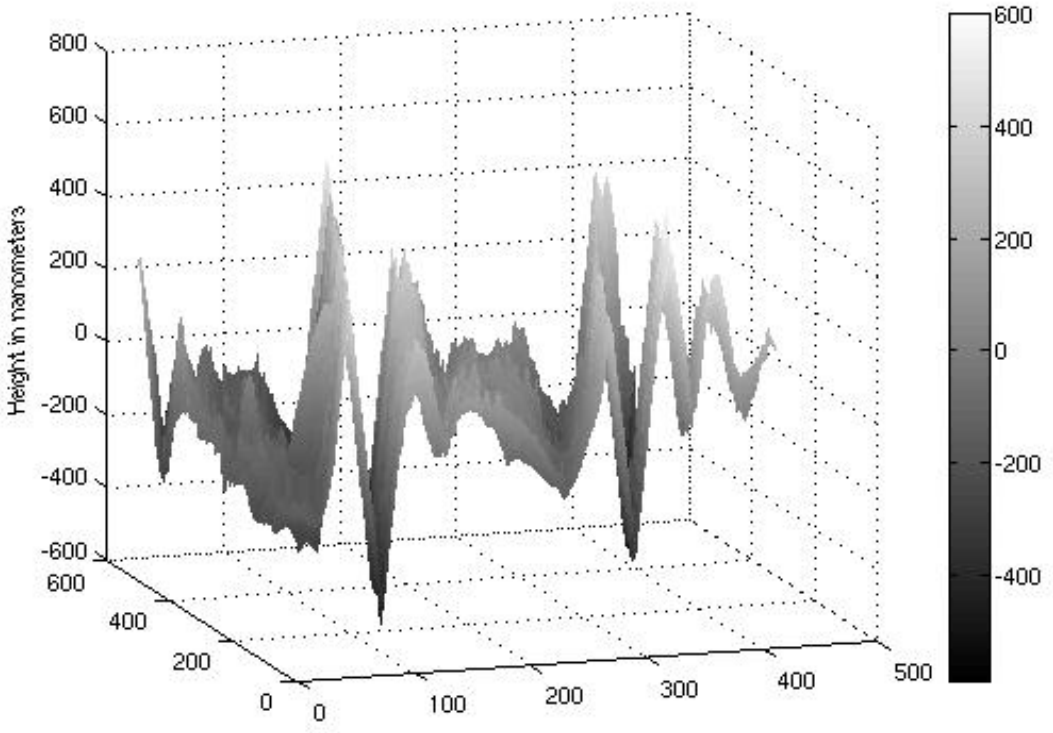

Fig. 13. KESM section profile measured in AFM viewed along the chatter lines.

It has been stated before that chatter artifacts limit the speed of sectioning and the thickness of the tissue section. Understanding how the artifacts vary depending on these parameters of the sectioning process is therefore vital to improve the sectioning process. Tissue samples sectioned in the KESM at speeds of 10mm/sec and 17mm/sec and section thicknesses of 2µm and 0.5µm were measured in the AFM, as shown in Figs. 14, 15, and 16. Table 2. gives the variation of the chip thickness and the distance between successive ridges for various samples from the KESM sectioning process.

Table 2. AFM measurements of KESM sections.

S. no	Desired chip thickness (µm)	Cutting speed (mm/s)	Distance between successive ridges (µm)	Variation in surface profile (nm)
1.	0.5	10	39.41	1000
2.	0.5	17	12.94	825
3.	0.5 (Block)	17	13.72	350
4.	2	10	8.31	1300

From table 2, it can be observed that

1. the frequency of the chatter (measured as variation in chip thickness) increases as the desired section thickness increases,
2. the variation in the surface profile, which represents the variation in chip thickness, increases as the desired section thickness increases,
3. the variation in the surface profile decreases as the sectioning speed increases.

Also, it has been observed that by varying tissue sectioning speeds in KESM, chatter can be suppressed. Hence, during normal operation in KESM, successive sections are cut at speeds varying as much as 2:1. Fig. 6 in Chapter III shows the cross section (X-Z) of the volumetric image data obtained by varying the sectioning speeds. As stated in Chapter III, the chatter artifacts in the image are aligned across successive sections with slow continuous shifts of phase irrespective of the varying sectioning speeds at random. This fact suggests that the chatter phenomenon in KESM can be attributed mostly to regenerative effects in the sectioning process. Geometric sectioning requires careful separation of tissue sections and measuring them using the AFM. Optical characterization offers a quicker alternative to speed up the process of analyzing and characterizing the sectioning process. Subsequent sections below give more

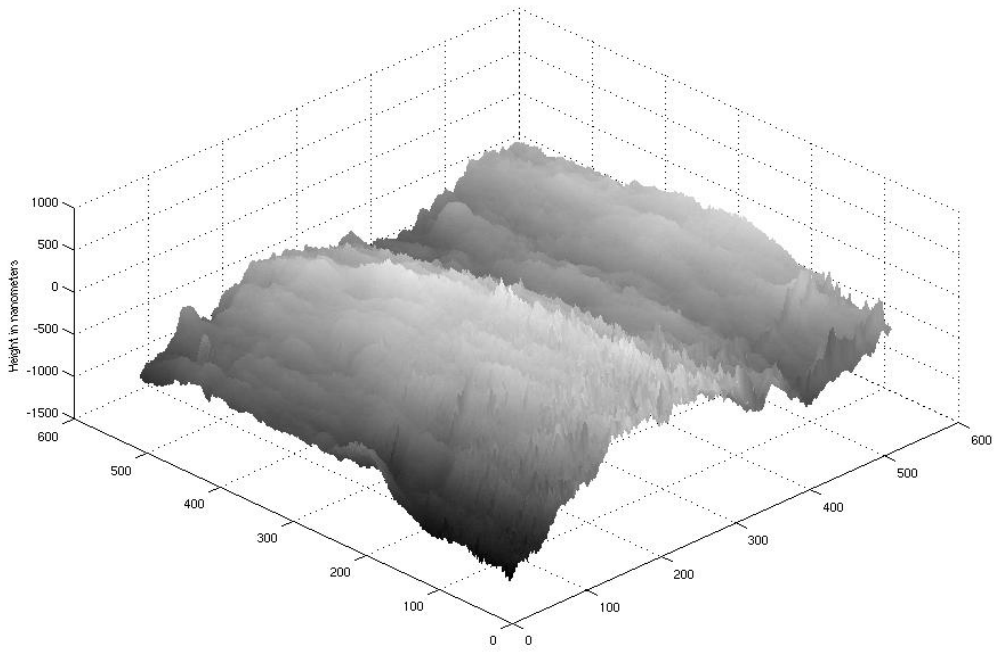

Fig. 14. Chatter in the section surface profile. Scan area was 90µmX90µm. Speed of cutting was 10mm/s. Average section thickness was 0.5µm. Surface profile varies as much as 500nm and the variation is smooth due to low cutting speed.

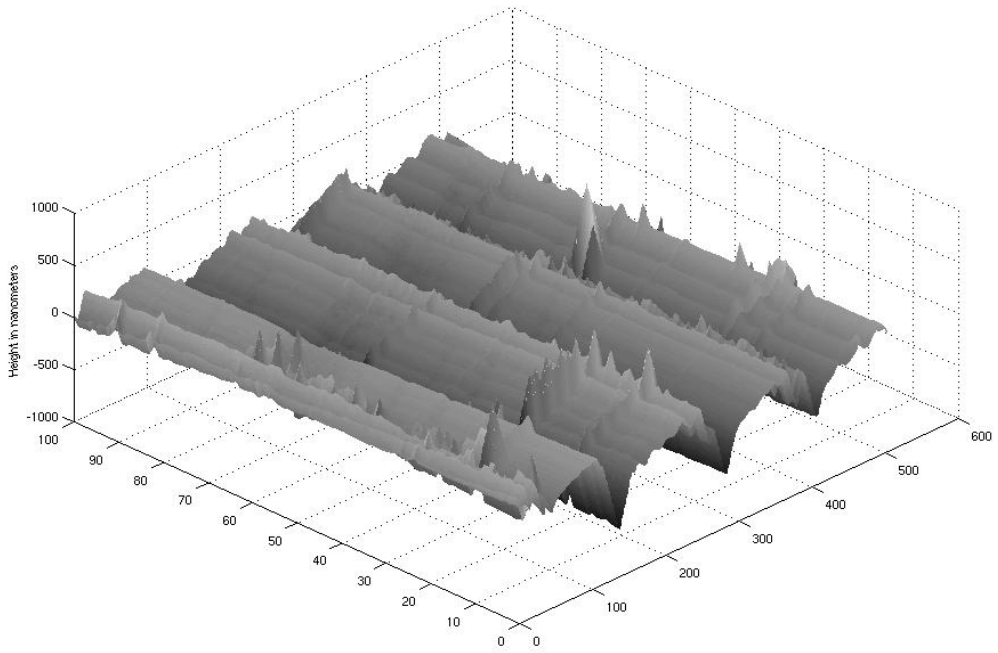

Fig. 15. Chatter in the section surface profile. Scan area was 50µmX50µm. Speed of cutting was 17mm/s. Average section thickness was 0.5µm. Four groves appearing on the surface profile correspond to section thickness variation due to chatter.

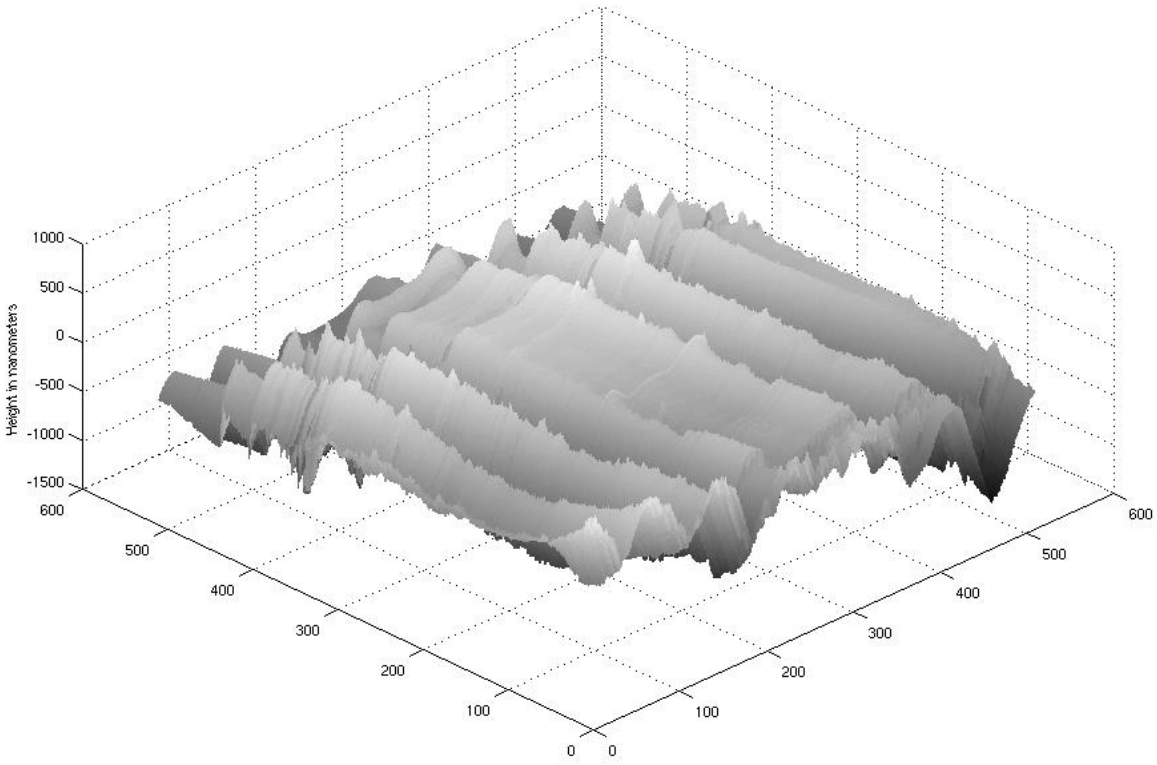

Fig. 16. Chatter in the section surface profile. Scan area was 50µmX50µm. Speed of cutting was 10mm/s. Average section thickness was 2µm. Section thickness variation due to chatter appears as grooves (six).

information about optical characterization.

G. Optical characterization

Instabilities in the sectioning process can be seen on the chip surface when viewed through a microscope. This technique of imaging the chip to inspect the quality of the surface is a standard technique in manufacturing processes. It gives a good qualitative measure of the sectioning process. In the KESM, this technique can be used to quantify the process as well. In biological tissue sectioning, the workpiece material is translucent plastic. White light is directed through the diamond knife, internally reflected within the knife, where it illuminates the chip at the edge of the diamond knife (Fig. 17). This back

illumination of the chip, while the section is passing over the knife edge, is used to image the section. Therefore, any variation in the thickness of the chip is reflected as variation in the brightness of the image. Hence, analyzing the volumetric imaging data in KESM-like instruments can be used to characterize the sectioning process as well.

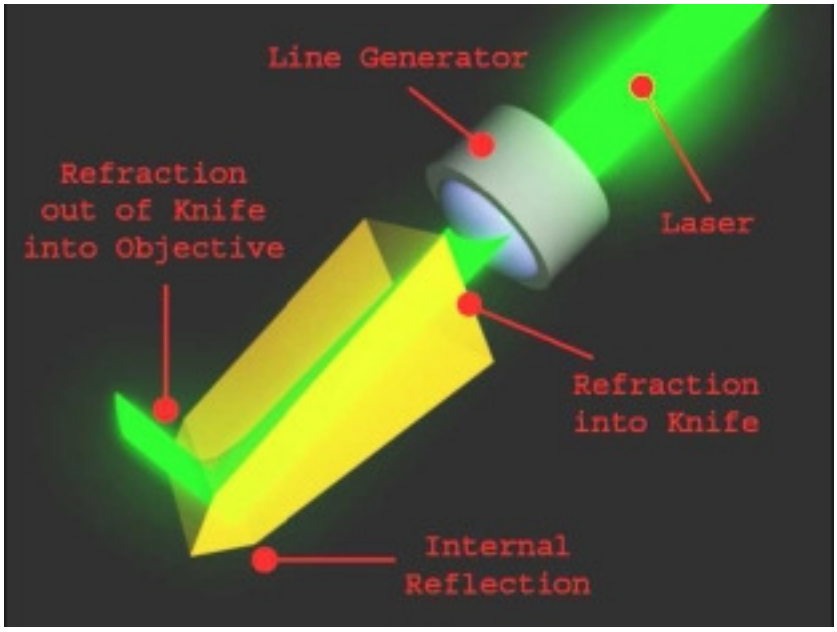

Fig. 17. Illumination mechanism of KESM. White light, directed through the diamond knife, is internally reflected to illuminate the section at the knife edge.

Chatter gives rise to non-uniform section thickness, which in turn appears as alternating dark and bright patches in the scanned image. These alternating bright and dark streaks are aligned across successive sections with more or less continuous phase shift (see Fig. 6, Chapter III). These observations are only possible due to simultaneous sectioning with back-lit imaging.

Fig. 18 shows the images obtained from the KESM while sectioning at thicknesses of 0.5um and 2um with sectioning speeds of 10mm/s, 17mm/s, and 20mm/s. From Fig. 18 it can be observed that the chatter artifacts decrease as the sectioning speed

increases and as the desired chip thickness increases supporting the observations obtained from the geometric characterization.

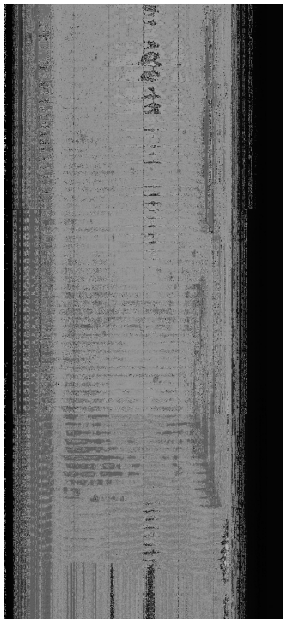	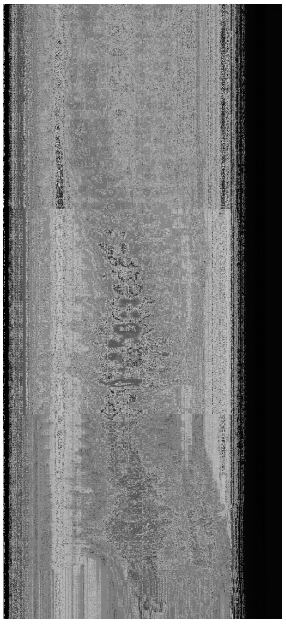	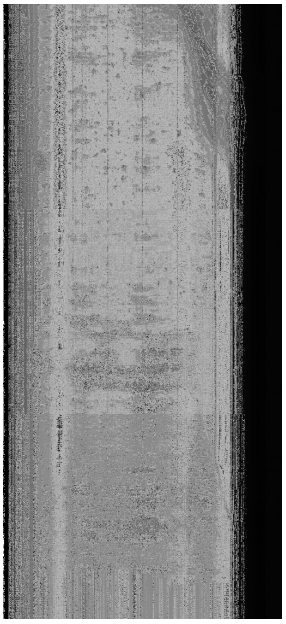
0.5µm at 10mm/s	0.5µm at 17mm/s	0.5µm at 20mm/s
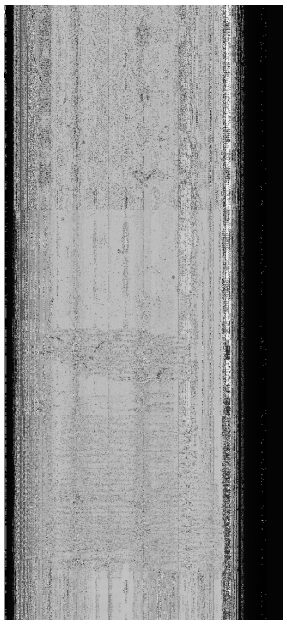	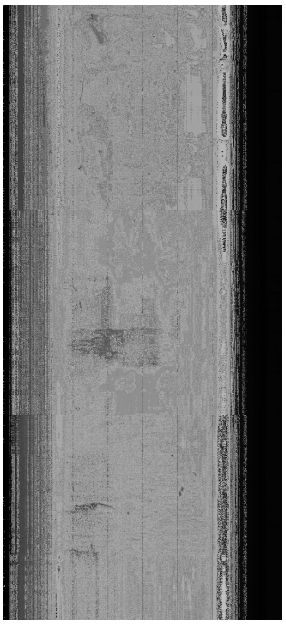	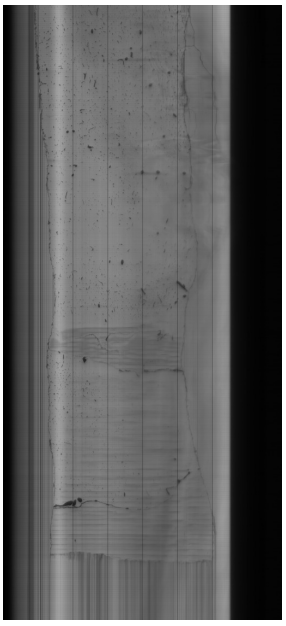
2µm at 10mm/s	2µm at 17mm/s	2µm at 20mm/s

Fig. 18. Image data recorded in KESM while cutting sections at 0.5µm and 2µm at sectioning speeds of 10mm/s, 17mm/s, and 20mm/s.

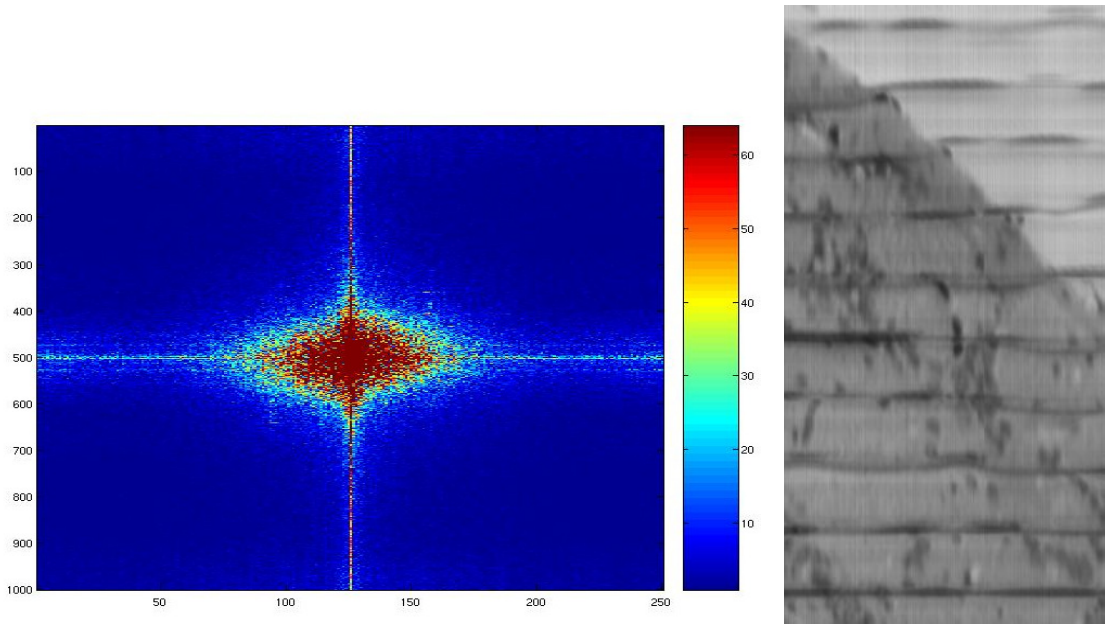

Fig. 19. KESM image with chatter and its corresponding Fourier transform.

Chatter always appears as streaks along the cutting or X-direction. Taking the Fourier transform of any image with chatter gives the frequency of chatter streaks in pixels. Fig. 19 shows an image with chatter and its corresponding Fourier transform (the Fast Fourier transform algorithm provided in Matlab was used). This image clearly shows that the dominant frequencies of the image occur when along the vertical direction. Lower frequencies in the image are equally distributed in both the X and the Y directions. Hence we can conclude that the lower frequencies belong to the structural information of the tissue section and moreover the chatter artifacts being strictly along X-direction; they appear in the Fourier image on the Y-axis only. This information can be used to extract various frequency modes in which chatter is active.

H. Summary

Chatter in the sectioning process limits the advantages of biological 3D microscopy using physical sectioning. Therefore characterization of the sectioning process in general and chatter in particular is required to understand and abate chatter and its limiting effects in volumetric data acquisition. This chapter has identified acoustic, vibration, and profile characteristics of chatter phenomenon and demonstrated measuring techniques for these characteristics. Measuring the vibration characteristic of the knife is discussed in detail in the next chapter. Other key parameters affecting the sectioning process are the mechanical properties of the polymer used to embed the stained tissue. Techniques to characterize such polymer properties are discussed in the Chapter VI.

CHAPTER V

VIBRATIONS IN THE KESM SECTIONING PROCESS

A. Introduction

The cutting tool in the sectioning process exerts force on the workpiece, which should equal the resistance offered by the workpiece material to cutting. This is the ideal case. Due to multitude of reasons and external disturbances, this seldom happens. If any of these opposing forces changes rapidly, the corresponding balancing force requires time to adjust to this change, and this delay induces a force imbalance in the system. Such small imbalances can induce undesired vibrations in the system, which either dampen out returning the machining process back to stability, or are sustained in the system, inducing chatter in the machining process.

B. Vibrations in the sectioning process

Unbalanced forces in the sectioning process result in the vibration in the cutting tool. These vibrations in the cutting tool are often reflected in the sectioning as grooves on the surface of the workpiece or on the chip. When the cutting tool passes over the groovy surface from the previous cut, it experiences rapid changes in the material resistance. Catching up to these fast variation in the opposing force requires time and hence requires a small time lag. During this lag, the forces are unbalanced, giving the knife some acceleration in the form of a jerky motion which results in uneven surface and this loop can continue forever. Such undesired vibrations can be captured in the variation

of the acceleration of the cutting tool, and therefore measuring the acceleration variation gives vital information about chatter in the sectioning process. This information can further be used in modeling and abating the chatter.

C. Experimental setup

The sectioning process in the KESM employs a diamond knife fixed to a bracket firmly attached to a massive granite base for stability. The workpiece (or specimen) is mounted within a *specimen tank* atop a 3-axes mechanical stage. The latter can be programmed to move to achieve cutting and concurrent imaging of the tissue sections. During each cut, the workpiece hits the diamond knife and gives an impulse to the knife. This impulse can induce as force imbalance, allowing undesired vibrations to creep in to the sectioning process. As mentioned in the previous section, these vibrations can be measured as changes in acceleration of the diamond knife.

Fig.20. PCB Piezotronics (TM) 352A24 shear accelerometer used to measure vibrations of the diamond knife during the sectioning process in the KESM [14].

An accelerometer is a device that measures the acceleration of itself, and can be attached to the surface of anything whose acceleration needs to be measured. To measure the acceleration of the diamond knife of the KESM, a shear accelerometer supplied by PCB Piezotronics (TM) (model 352A24 (Fig. 21)) has been used. It is a light weight accelerometer (0.8gm) with sensitivity of 10.2mV/(m/s²) with +/- 10% accuracy. It can

measure accelerations of up to +/-490m/s². Readings can be taken up to a maximum of 8000 samples per second with +/-5% error. The accelerometer is attached to a 10ft cable ending in a BNC connector. Since the voltage generated by this accelerometer is generally feeble, it is amplified further by a signal amplifier supplied with the accelerometer. Output from the amplifier is plugged in to a National Instruments BNC 2110 board, which in turn is connected to a Dell Power Edge Server through a National Instruments PCI 6415 card. National Instruments (TM) Labview Signal Express software was used to acquire the data from the accelerometer at the maximum sampling frequency of 8000Hz. Fig. 20 shows the block diagram of the setup to measure acceleration of the KESM knife.

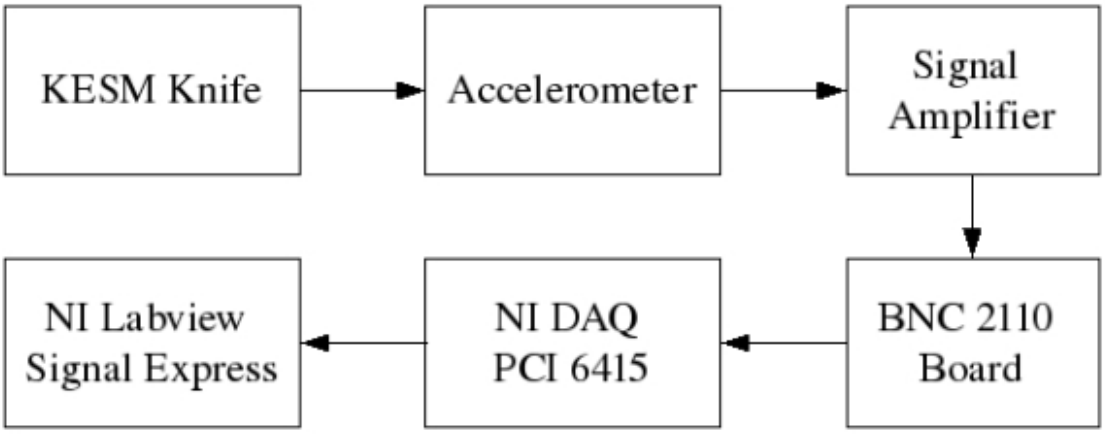

Fig. 21. Block diagram of the setup to measure acceleration of the knife in KESM.

The diamond knife assembly in the KESM is mounted in such a way that the knife and the bracket holding it should remain static even while the sectioning is taking place. But this does not hold in reality. As the workpiece moves towards the diamond knife for sectioning, it gives an impulse to the knife at the moment of contact and this impulse initiates vibration in the knife. These small induced vibrations subsequently give rise to chatter. Measuring these vibrations as acceleration of the diamond knife provides insight

the chatter process and its dynamics. To measure the acceleration of the knife, the PCB accelerometer was mounted on the bracket holding the knife. This accelerometer measures the acceleration in only one direction -- in the cutting direction. This choice of axis can be justified by the observation that chatter streaks in KESM image data are perpendicular to the direction of cut.

D. Vibrations in the KESM knife

Acceleration measurements, along with the image data, were taken during successive sectioning strokes of the KESM. Fig. 22 shows the acceleration recorded by the accelerometer fixed to the bracket holding the knife. The knife-bracket joint is rigid and hence the acceleration of the knife can be safely assumed to be the same as that of the bracket. Measurements were taken during tissue sectioning for a period of 100 seconds, during which 19 sections were cut. The acceleration of the knife significantly increased during each sectioning stroke and the number of such changes is equal to the number of sections cut during the time of measurement. The high amplitude of the acceleration is due to chatter. During chatter-free sectioning in KESM the acceleration variation is smaller and is mainly due to the initial impact of the workpiece against the knife.

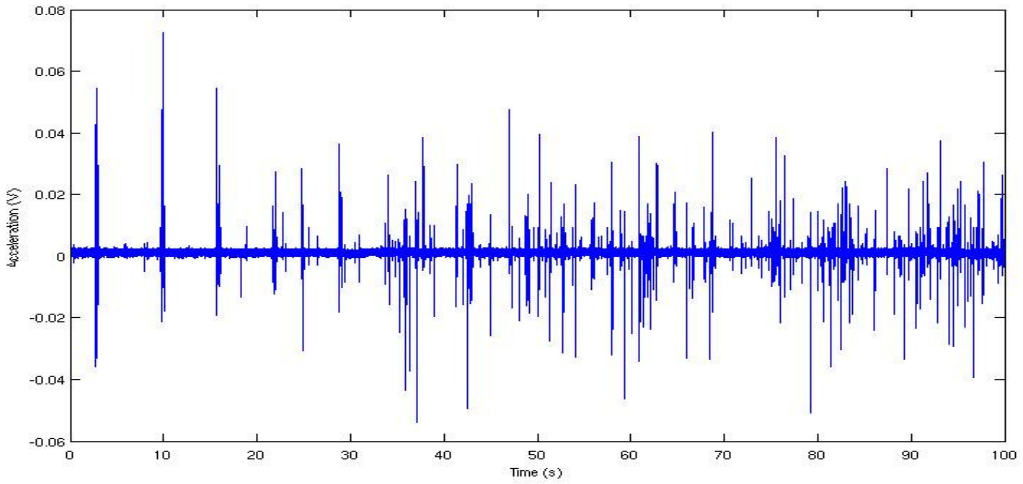

Fig. 22. Acceleration of the diamond knife of KESM during tissue sectioning as a function of time. Total number of sections cut during this time period was 19. Accelerometer sensitivity is 10.2mV/(m/s²).

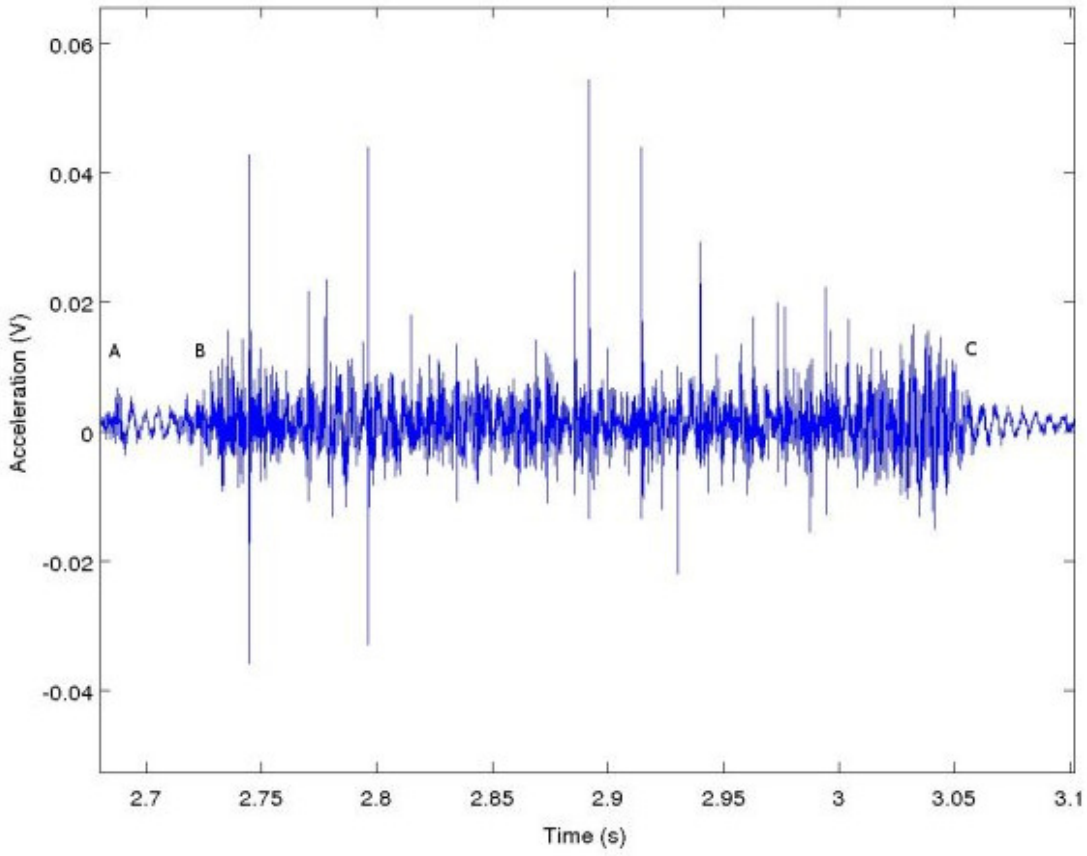

Fig. 23. Acceleration of the diamond knife of KESM during one sectioning step. A. Workpiece comes into contact with the stationary diamond knife. B. Chatter begins. C. Workpiece loses contact with the knife.

Taking a closer look at the acceleration during one particular sectioning stroke reveals the stages of chatter generation. Fig. 23 shows the acceleration of the knife during one such cut. It reveals how the forces act at on the knife during various phases of the cutting process. As the workpiece first comes in contact with the diamond knife, it exerts an impulse on the knife, which then vibrates, as shown as 'A' in Fig. 22. The acceleration profile is similar to the force vibrations, which then become much more erratic. This marks the beginning of the chatter, shown as 'B' in Fig. 22. Chatter continues as the knife sections the workpiece till 'C' in Fig. 22, after which the knife loses contact with the workpiece and the acceleration of the knife dampens down.

It can be observed that the profile of the acceleration variation of the knife (Fig. 23) is similar to the chip thickness variation, as measured in the profilometer as shown in Fig. 13 in Chapter IV. This strengthens the proposition that regenerative chatter arises from the uneven surface of the workpiece, and this later is the major contributor of the chatter in the KESM.

The total time of the jitter, as seen from the acceleration measurement, can be calculated from Fig. 23 as approximately 0.4s. This time interval matches with the time interval of sectioning calculated from the imaging system. Each sectional image captured by the KESM optics is 9000pixels along the cutting direction and each pixel corresponds to 0.71µm. With a sectioning speed of 16mm/s, it takes 0.399s to cut the section that long. This close match of the time intervals indicates that the jitter in the diamond knife are due to sectioning and they dampen down once the workpiece loses contact with the knife. This also assures that the regenerative effect of chatter in the KESM sectioning process is not due to the undamped vibrations in the knife from the previous cut.

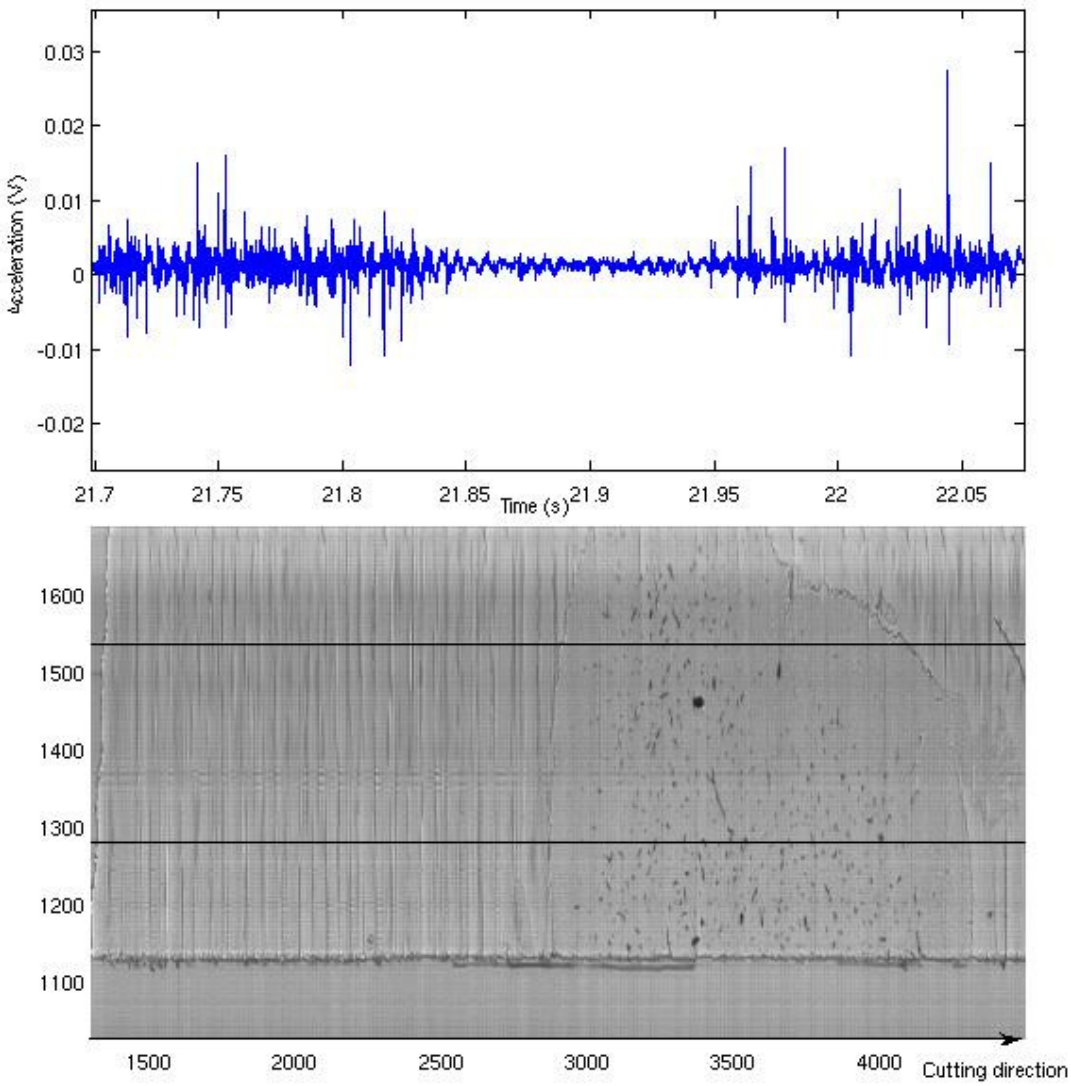

Fig. 24. Acceleration of the knife edge aligned with the image data of the section. Note that the chatter amplitude drops drastically when the softer tissue is sectioned by the knife compared to harder plastic. From time 21.85s to 21.95s in the top plot corresponds to the portion in the bottom image with an embedding tissue (3000 to 4300 along the X-axis).

Fig. 24 shows the acceleration of the diamond knife of the KESM while cutting a section with embedded tissue in the middle of the chip. Even though this acceleration measurement was taken while cutting a single section, there are two separate acceleration jitters in the knife. The corresponding image data for this acceleration measurement of the knife is also shown in Fig. 24. Comparing the acceleration data along side the image data

shows that the chatter amplitude dropped down while the diamond knife was sectioning the softer tissue, compared with its amplitude while sectioning the harder embedding plastic. This is in accordance with the fact that softer materials have a greater damping coefficient to absorb any undesired induced vibrations and therefore keep the chatter amplitude lower [9]. But to section thinner slices of the tissue, we need a harder plastic to embed the tissue. These conflicting requirements need to be satisfied by choosing an optimally hard embedding material.

Dominant frequencies that contribute to the knife chatter are revealed by a spectral analysis of knife acceleration. Fig. 25 shows the frequency spectrum of the acceleration of the diamond knife of KESM for different intervals during the sectioning process. When the knife is idle between the sectioning stroke, the dominant frequency occurs at 120Hz. This cannot be due to noise as the frequency is consistent across all intervals between the sectioning strokes. During the sectioning stroke, irrespective of whether the knife is sectioning the tissue or the plastic, the dominant frequency occurs at 170+/-5Hz. This suggests that the natural frequency of the knife might be 120Hz whereas the frequency of the chatter in KESM is close to 170Hz. Chatter artifacts in the corresponding image data occur at regular intervals of 130px (on average over 5 locations). This corresponds to the frequency of 173.34Hz for the sectioning speed of 16mm/s. Close match between these two frequencies affirms the fact that the vibrations in the diamond knife temporally correspond to chatter artifacts in the image date of KESM. The other dominant frequency at 480Hz is a harmonic and is also the second-most dominant frequency in the chatter artifacts of the image data. This supports the fact that the vibrations of the diamond knife are responsible for chatter in the imaging data of KESM. Also, as shown in Fig. 24, drop in the amplitude of the chatter while sectioning the embedded tissue is reflected in the

corresponding image data as well.

Knife idle	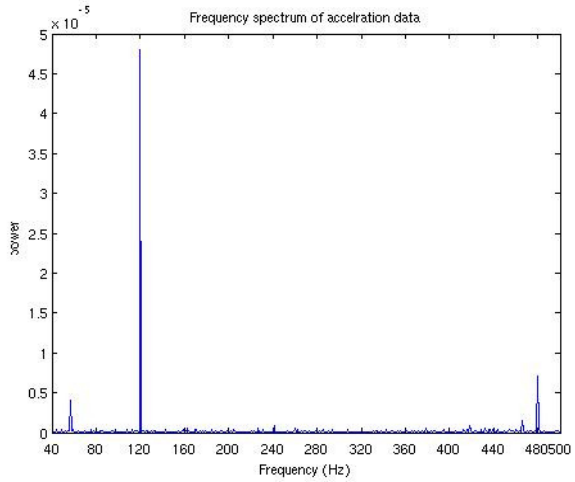
Knife sectioning plastic	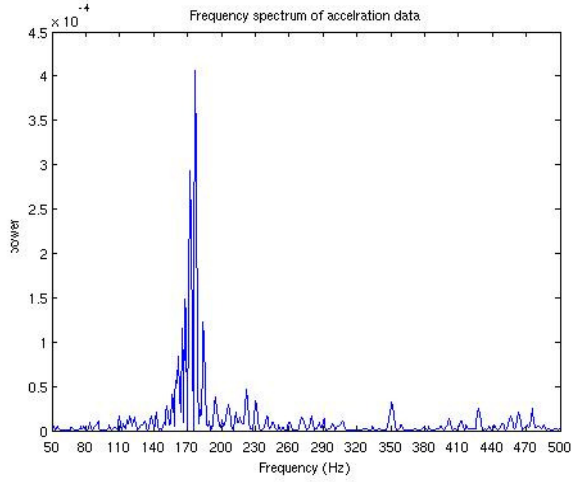
Knife sectioning embedded tissue	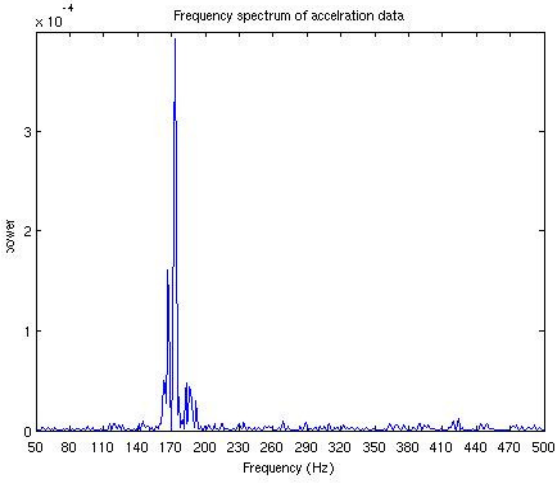

Fig. 25. Frequency spectrum of the acceleration of the diamond knife measured during sectioning in the KESM at different intervals.

E. Summary

In any machining process, the cutting tool exerts the force on the workpiece material to remove material and the workpiece material offers a resisting force. During machining, these forces are almost balanced. In reality, many undesired external and internal disturbances creep into the system, disturbing this force balance. This results in the vibration of either the cutting tool or the workpiece or both, thereby decreasing the machining quality. Measuring these vibrations in the sectioning process therefore helps in understanding and subsequently abating them.

Tissue sectioning process in KESM also suffers from these undesired vibrations called chatter. The diamond knife of KESM vibrates due to the impact with the workpiece resulting in uneven cut and hence an uneven workpiece surface. These vibrations of the knife were measured using an accelerometer. Matching the variation in the acceleration of the diamond knife against KESM tissue imaging data indicates that softer tissue sections tend to absorb the vibrations, decreasing the amplitude of the chatter, where as the harder embedding plastic increases their amplitude. Spectral analysis of the acceleration of the diamond knife reveals that the chatter artifacts and the vibrations share the same dominant frequency and therefore real-time acceleration readings can be used to find the frequency of the chatter artifacts and subsequently aide in their removal, as discussed in Chapter VIII.

CHAPTER VI

POLYMER CHARACTERIZATION

A. Introduction

Mechanical properties of the workpiece material play an important role in any machining process. Therefore, material properties for all metals are measured, standardized, and used frequently in the design of manufacturing processes [15]. Though equally applicable, no comparable tradition holds for the biological sectioning process. The embedding plastic/polymer, which is the base of the workpiece in biological sectioning, plays a vital role in the tissue sectioning process. It is therefore necessary to measure these polymer material properties and understand how they affect the process. Sections with good quality requires a careful choice of embedding plastic.

B. Mechanical properties

Machining, the oldest and most basic manufacturing process, has been the most studied of the mechanical processes. Material properties occupy an important aspect in machining, and many standard measurable properties have been identified, defined, and instruments have been developed to measure these mechanical properties of materials. The most fundamental material property is the reaction of the material to applied force. For standardization and comparison, *stress, the force per unit area*, represents the force, and *strain*, *the ratio of deformation to the original dimension,* represents the material reaction. Most measuring techniques involve applying stress to the material and

measuring the reaction of it as strain or deformation, giving rise to the 'stress-strain curve' of that material (Fig. 26). This curve represents the mechanical aspects of the material for most practical purposes. This curve also gives the elastic moduli, like Young's modulus and shear modulus of that material. *Young's modulus* is defined as the ratio of tensile stress to tensile strain. This represents the tendency of material to deform along the direction of force. Young's modulus typically remains constant for a particular range of stress. *Shear modulus* is similarly defined as the ratio of shear stress to shear strain. It represents the tendency of the material to shear when opposing forces are applied with a moment.

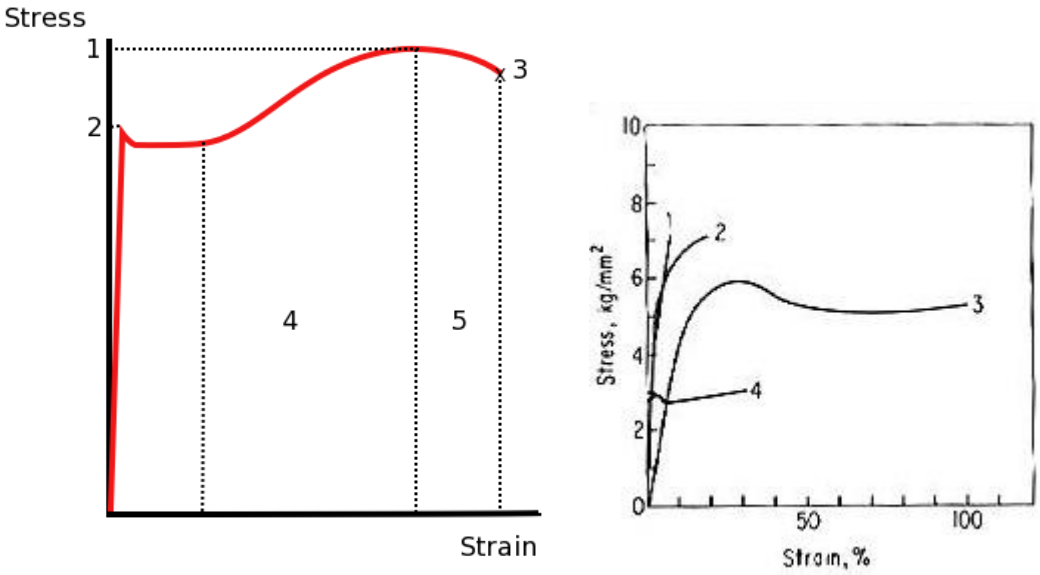

Fig. 26. A typical stress-strain curve (left) and measured stress-strain curve of thermoplastics [9] (1. Ultimate Strength 2. Yield Strength 3. Rupture 4. Strain hardening region 5. Necking region).

Hardness, the resistance of the material to plastic deformation, is another characterizing parameter for materials. It is defined usually by indentation [16]. Materials with high hardness resist more to deformation. The cutting process involves plastic

deformation of the workpiece material, so hardness of the material indicates the resistance it offers during the process of cutting.

For biological sectioning, epoxy resins, after paraffin, are the most used embedding polymers. Based on the choice of manufacturer and the setting process, these resins are called *Araldite* or *Epon*. Since the setting process of the resins influence their material characteristics, each setting protocol results in a material with different mechanical characteristics. Hence, for each polymer and setting process, there is a need to measure the stress-strain curve and the hardness of the resins to model the sectioning process accurately.

C. Techniques of measurements

Measurement techniques differ based on the material whose properties are to be measured and the scale at which the properties are to be measured. Physical tissue sectioning for biological microscopy involves cutting the specimens at the nanometer level and the tissue, being soft, is embedded often in paraffin or polymers. Based on these characteristics, we need instruments that are appropriate to measure properties of polymers at nanometer scales. The Digital Durometer and Nanoindenter are two such types of instruments. A *Digital Durometer* is an instrument that is widely used to measure hardness of soft specimens like plastics. A *Nanoindenter* is a nano-mechanical test system that is ideal for measuring elastic modulus and hardness of thin films.

D. Digital durometer

Durometer hardness testing is an international standard for hardness testing described in American Society for Testing and Material specification (ASTM) in D2240

[17]. Along with the Rockwell hardness test, it is the most commonly used test to measure the hardness of plastics. Durometer also refers to the instrument used to measure hardness. Durometers (instrument), invented by Albert F. Shore, come in different scales based on the material hardness, of which A and D are most common. Scale A is used for soft plastics, while scale D is used for hard plastics. Durometer hardness values are on a scale of 0 to 100. Hardness of a given specimen is measured by applying indentation load on the specimen. Though the Durometer reading gives the resistance of the specimen to indentation load, predicting other material properties using only this is often inaccurate. On the whole, Durometers provide an easy and fast way to measure hardness of specimens without prior preparation.

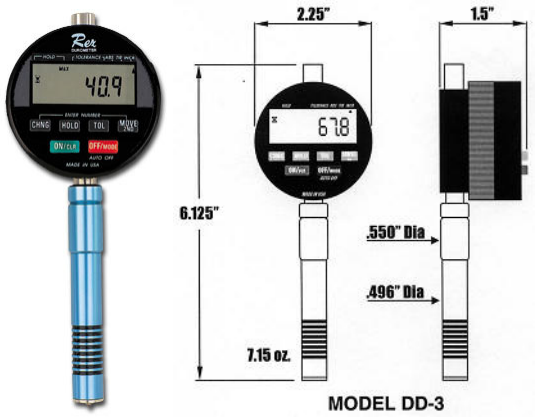

Fig. 27. Rex DD-3 digital durometer (Left) and its model diagram (Right) [17].

For our experiments, the Rex(TM) Digital Durometer of scale D, shown in Fig. 27, was used to measure the hardness of Araldite and Epon. Measurements were taken on both pure plastic and tissue embedded in the plastic. The durometer readings for clear plastic (both the Araldite and the Epon) vary between 80 and 85. For tissue embedded in the plastic block, the durometer reading drops down to 70+/-5. This indicates that the part

in the workpiece containing embedding tissue is much softer (in terms of the durometer hardness) than the part of the workpiece containing pure plastic, predicting variation of the knife acceleration while sectioning the workpiece.

E. Nanoindenter

A Nanoindenter is a nano-mechanical test system for measuring the mechanical properties of thin specimens, and is used to characterize the mechanical properties of materials at nanometer length scale. Force versus displacement response of a specimen is obtained by indentation on the surface by a diamond probe. Elastic modulus and other material properties can be determined from this response. We used the Hysitron TriboIndenter (Fig. 28), available at the Material Characterization Facility (MCF) at Texas A&M University. This particular nanoindenter has a load resolution of less that 1nN and displacement resolution of 0.0002nm [18].

For our experiments, we used the TriboIndenter to measure the material response for an applied force. Material properties sometimes vary at smaller thicknesses, sometimes as much as ten-fold from their bulk properties. Taking that into account, we used 1µm thick sections to measure the response. Araldite and Epon, the base polymers for embedding the tissues for the KESM, were measured. The tip of the TriboIndenter's diamond probe applies an increasing force, starting from 0 to 1000µN on the section, and the displacement of the tissue is measured at nanometer accuracy. This response of the specimen to applied force can be used to evaluate the stress-strain curve and elastic moduli of those materials.

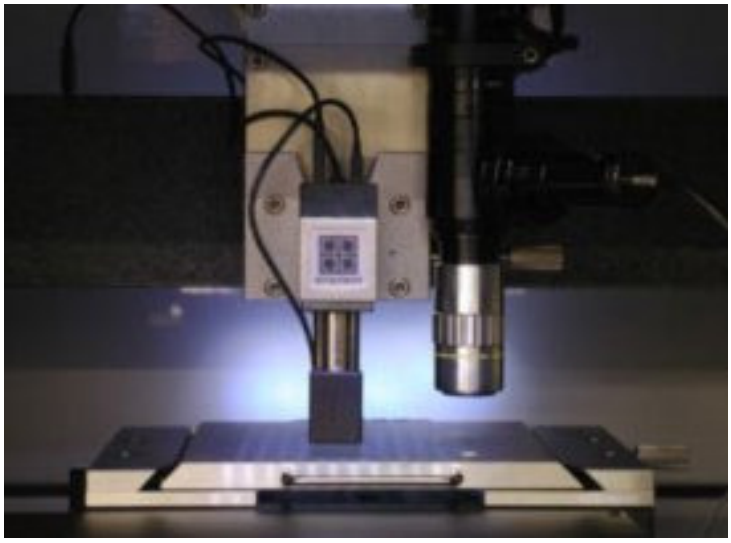

Fig. 28. Histiron Triboindenter. Test bed on the stage, and the transducer and the optical viewer are visible in the picture [18].

TriboIndenter measures the material response at a series of points arranged as a rectangular array. As the instrument is used for nano-scale response, multiple readings are necessary to prevent errors from external disturbances. We took the set of 9 readings, each at a different location. These measurement locations were arranged as a series of 3 lines. Fig. 29 shows the TriboIndenter data for Araldite and Epon with 9 sets of measurements.

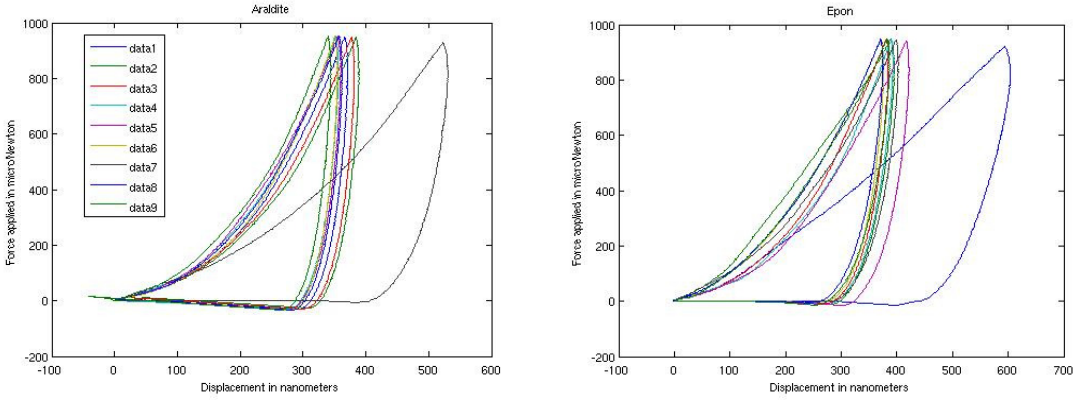

Fig. 29. TriboIndenter readings of Araldite (left) and Epon (right).

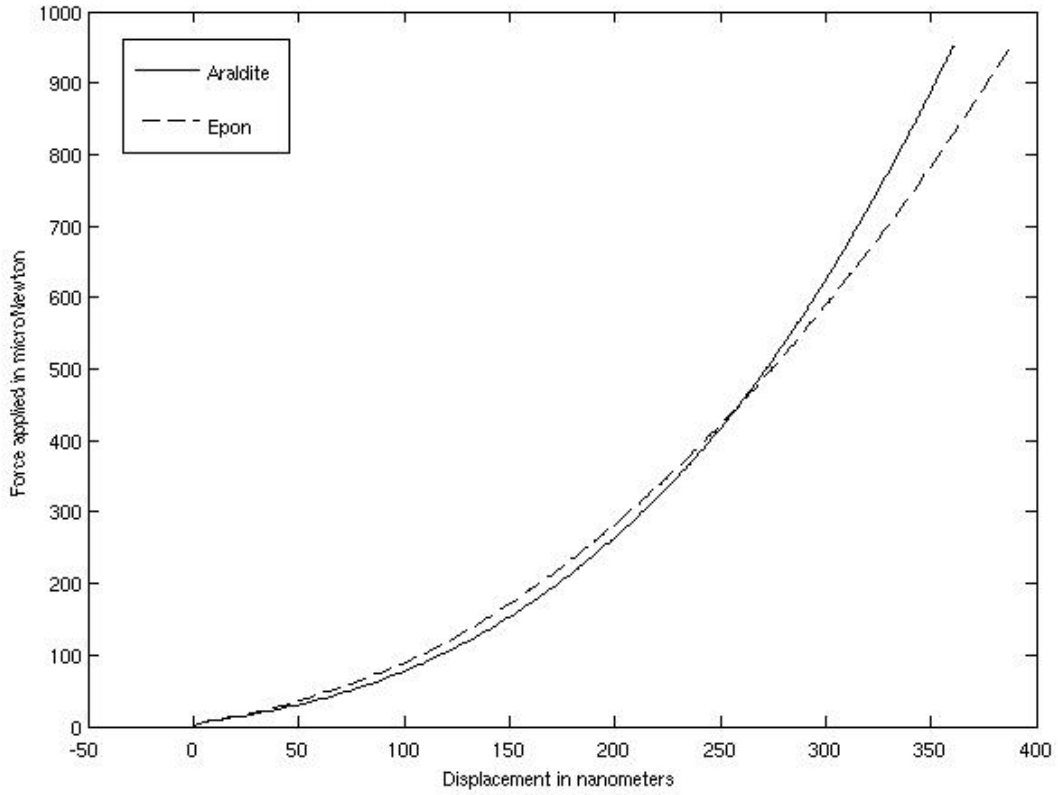

Fig. 30. Average force vs. displacement response of Araldite and Epon resins. Force is applied on each specimen starting from 0 to 1000μN and the corresponding displacements were measured in nanometers.

Responses of the materials were obtained by removing measurements that differ most from the rest and then averaging the remaining readings. Fig. 30 shows the average response plot of Araldite (solid line) and Epon (dashed line) for the applied force. This material response data directly corresponds to the stress-strain curves and elastic moduli of Araldite and Epon, and can be used either to model the process or to compare various plastics that can be used as an embedding medium for biological tissue sectioning.

F. Summary

Mechanical properties of the workpiece material determine the forces exerted by the cutting tool in any sectioning process. Response of the material to an applied external stress in terms of strain, called the “stress-strain curve”, is considered to be the most

important among such material properties. Stress-strain curve of any material gives various elastic moduli, which determine how the material responds to different forces. Hence, this measurement forms a vital part in designing any machining process. Material hardness, which is easier to measure, is another material property which can be used to quickly compare different embedding polymers based on how they react to indentation.

Measuring these two properties of any material, various design parameters of the machining process can be chosen. In the KESM, the workpiece contains stained tissue embedded inside a block of Araldite or Epon. The properties of these resins determine the forces in the sectioning process and thereby the sectioning parameters. A digital durometer has been used to measure the hardness of these materials and the embedded tissue, and gives a quick estimate of how hard the embedding polymers are compared to the tissue. Later in this thesis, these values, along with the image data and the knife acceleration data, are used to understand how the workpiece material affects chatter in the sectioning process of the KESM. To measure the response of these embedding polymers as thin sections, the technique of nano-indentation has been used. Nano-indentation gives the specimen material's mechanical properties at nano-scale as the response of the material to an applied external force. Measurement has revealed that the embedded tissue is much softer than both the embedding polymers, and the material response of the Araldite and the hard Epon do not vary significantly.

CHAPTER VII

NONLINEAR DYNAMICAL MODELING OF THE CUTTING PROCESS

A. Introduction

In this chapter we will review some standard models of cutting process and chatter mechanism. We discuss the applicability of these models to biological sectioning process and then extend it to fit the sectioning model of KESM.

B. Sectioning process

Cutting process is a fundamental and most widely used machining technique and hence the most studied process. Orthogonal cutting process is the simplest of all cutting processes where the cutting tool has its cutting edge perpendicular to the relative velocity between the tool and the workpiece. Fig. 30 shows a typical orthogonal cutting process. The process of chip formation even in the orthogonal cutting process involves a complex interplay of the cutting tool, the workpiece, and the chip dynamics. This makes the task of modeling the cutting process complex and none of the models developed so far can fully state a complete and correct solution. But these various models helped in the analysis of certain phenomenon which helps in directing the choice of parameters to improve the cutting process. A simplified model involves two-dimensions and assumes a thin shear zone. Experimental evidence suggests that the thin shear zone model describes the process accurately during high cutting speeds whereas the thick shear zone model is accurate for low cutting speeds [9].

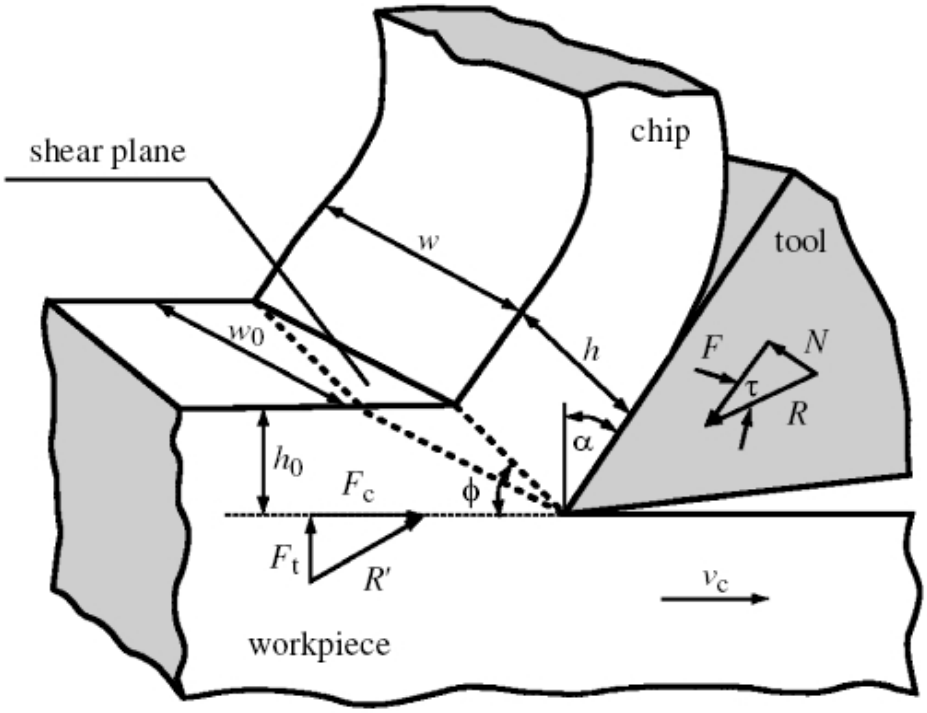

Fig. 31. Orthogonal cutting process model [7].

Fig. 31 shows the orthogonal cutting process with various forces and angles involved. The cutting tool exerts a force R on the workpiece material to counter the resistance R' offered by the workpiece. As the speed of cutting is constant, R and R' should be equal and act in opposite direction. Using the free body diagram, shown in fig. 32, we can find these basic forces acting in the system.

C. Cutting models

Force R exerted by the cutting tool on the workpiece can be divided into two components: (1) cutting force (Fc) acting in the direction of cutting and (2) thrust force (Ft) acting in the direction perpendicular to cutting direction. Similarly, the resistance offered by the workpiece R' can be divided into two components: (1) shearing force (Fs) acting along the shear plane and (2) frictional force (Ff) acting along the surface of the

tool flank. When the clearance angle, shown in Fig. 31, is small, an additional frictional force can act on the cutting tool due to the contact between cut surface of the workpiece and tool.

The tool flank is at an angle to the vertical which is termed the rake angle (α). Rake angle can be either positive or negative or zero depending on the process requirements. The angle between the direction of chip flow and the cutting direction is called shear angle (ϕ). Shear angle is considered the most important factor in any process where the cutting is achieved by a shearing process. It is non-trivial to measure the shear angle and hence various approximations are used in different models. Friction angle τ (shown as β in the Fig. 32) is another important parameter in the cutting process. It is the angle between the direction of the frictional force on the tool flank and the resultant force R. With the basic terminology defined, we will now look into various models of orthogonal cutting process.

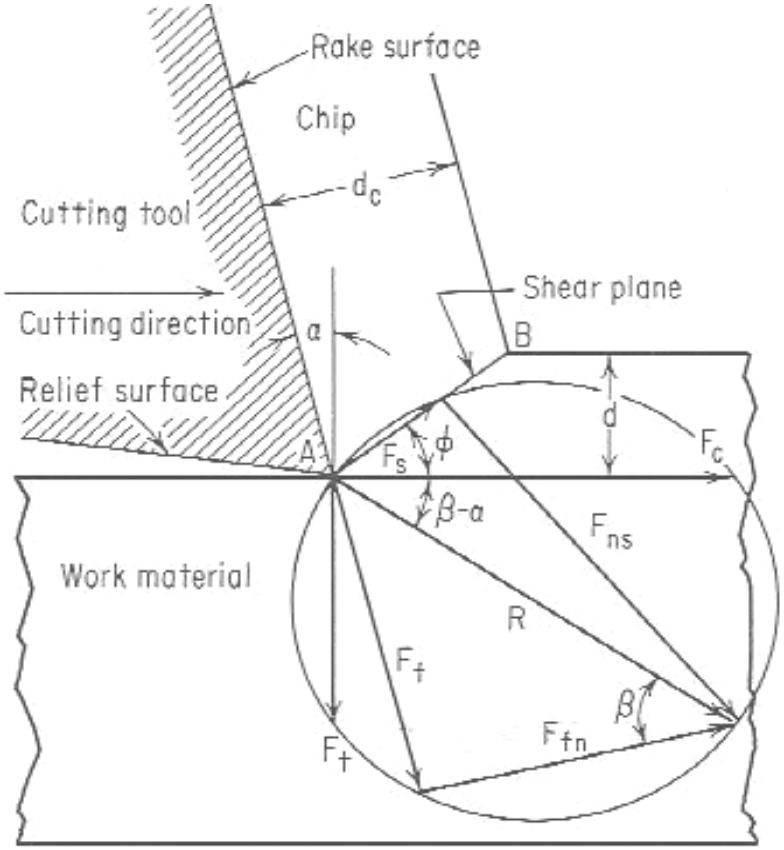

Fig. 32. Force diagram of the orthogonal sectioning process [9].

D. Merchant's model

One of the earlier models of metal cutting process was given by Merchant et al. [18]. It described the process in terms of chip formation. The main assumptions of this model include continuous flow of the chip, thin shear zone, and invariance of the width of the chip. Forces involved in this model are the cutting force exerted by the tool, the shear resistance by the work piece, and the frictional force between the chip and the tool flank (Fig. 32). Balancing these forces gives us

$$R = \frac{F_s}{\cos(\tau - \alpha + \varphi)},$$

where the shearing force Fs is defined as

$$F_s = \sigma_s A_s .$$

Here, σs is the shear stress and As is the cross-section of the shear plane which can be expressed in terms of the chip width and the depth of cut as $A_s = \frac{wh_0}{\sin\varphi}$. By substituting As in the expression for Fs, we obtain R as

$$R = \frac{\sigma_s w h_0}{\cos(\tau - \alpha + \varphi)\sin\varphi} .$$

We can now express the components Fc and Ft of R as

$$F_c = \sigma_s w h_0 \frac{\cos(\tau - \alpha)}{\cos(\tau - \alpha + \varphi)\sin(\varphi)} = \sigma_s w h_0 \frac{\cos(\tau - \alpha)}{\sin^2(\varphi)} ,$$

$$F_t = \sigma_s w h_0 \frac{\sin(\tau - \alpha)}{\cos(\tau - \alpha + \varphi)\sin(\varphi)} = \sigma_s w h_0 \frac{\sin(\tau - \alpha)}{\sin^2(\varphi)} .$$

Merchant's model assumes that the shear angle is based on the minimum energy principle as $\phi = \frac{\pi}{4} - \tau + \alpha$. This gives us the above expressions for cutting and thrust forces. This model depends upon shear angle ϕ and other parameters are given as functions of ϕ. By determining the quantity to minimize, we can find an optimum shear angle for the cutting process.

E. Kudinov's model

Kudinov developed another model of orthogonal cutting process in 1955 [7] using dynamic cutting characteristics to explain chatter. In his model, the expression for the cutting force Fc is taken empirically [7] as

$$F_c = C_c \sigma_s w \xi h_0 ,$$

where C_c is material constant, σ_s is the shear stress, and $\xi=h/h_0$ is the ratio of chip thickness. If we assume that the material properties remain the same, we can obtain the cutting force dynamics by differentiating above expression for F_c with the remaining variables h and ξ which gives

$$dF_c = C_c \sigma_s w \left(\xi dh + h_0 d\xi \right).$$

From Fig 32, chip thickness ratio can be calculated as

$$\xi = \cot\varphi \cos\alpha + \sin\alpha .$$

By balancing the forces in the shear plane and rake surface, Zorev obtained the following [7]:

$$l = \frac{s_R l}{s l_R} \left(\tan\tau + \tan\left(\varphi - \alpha\right) \right) h .$$

Using these models, Wiercigroch & Budak [7] obtained the force dynamics as

$$dF_c = C_c \sigma w \left(\xi_0 dh + h_0 \left(\frac{m}{n} \right) \left(\frac{\xi_0}{v_c} \right) d^2 h \right),$$

$$dF_t = C_t \sigma w \left(\xi_0 dh + h_0 \left(\frac{m}{n} \right) \left(\frac{\xi_0}{v_c} \right) d^2 h \right),$$

where C_t is the thrust force constant. These force dynamics give a basic model of the orthogonal cutting process which can account for chatter generation as nonlinearities in the metal cutting process model.

F. Models of chatter generation

As defined in the earlier chapters, mechanical chatter is an undesired vibration in cutting tool or workpiece during the cutting process. It is a self-sustaining process and can continue unless quenched. In machining processes like milling and cutting, the effects of chatter are visible as lines or grooves on the surface of the workpiece. Usually, these lines or grooves are regularly spaced along the direction of cutting. The distance between them depends on the frequency of the knife or the workpiece vibration and the cutting speed.

Chatter limits productivity and quality of machining process and with ever increasing cutting speeds this has become a major problem in metal cutting. This lead to modeling and analysis of chatter since late '50's. Initial modeling techniques studied chatter in orthogonal cutting and identified the machine tool dynamics and the feedback from the cutting surface as primary sources for this phenomenon. These studies have a fundamental limitation of temporal invariance of chip thickness. Wiercigroch and Budak identified four different mechanisms of machining chatter based on the source of chatter generation: (1) friction, (2) regeneration, (3) mode coupling, and (4) thermo-mechanics of chip formation [7]. These different mechanisms can act together, further complicating the task of modeling.

Frictional chatter, as the name indicates, is due to the friction force. In orthogonal cutting, friction can exist between any surfaces in contact with relative motion such as work piece-tool flank and chip-rake surface. This force depends on the cutting velocity. Wiercigroch and Krivstov [19] showed that even a system with one DOF can give rise to frictional chatter.

Regenerative chatter is a self-induced vibration due to repeated cutting of an uneven surface. This type of chatter is self-sustaining due to the fact that cutting an

uneven (wavy) surface induces oscillation in cutting force magnitude. This oscillating cutting force results in uneven (wavy) surface again, often with an increase in the amplitude. Effectively, the chip thickness depends on the cutting force which in turn depends on the thickness of the chip at some time in the past. Delay differential equation (DDE) provides a good mathematical model for this kind of system. DDEs spring up often in control systems and are studied extensively in control theory.

G. Stepan's model of regenerative chatter in metal cutting

Stepan applied the simplified one-dimensional DDE model to the regenerative chatter and studied the stability of that system [20]. His model assumed that the cutting force dynamics can alone determine other nonlinearities occurring in the sectioning process and got away with other variations.

Using the experiment-based approximation of the cutting force, called the three-quarter rule, Stepan used the following function to capture the dependence of the cutting force on the width of the chip (w) and the thickness of the chip:

$$F_c = c_1 w h^{3/4},$$

where c_1 is a constant. Note that the dependence of the cutting force on the cutting speed is neglected in the above approximation. Using the experiments and simulations done by Usui, Davies, and Marusich, Stepan derived the expression for the cutting force as:

$$\Delta F_x = k_1 \int_{-\sigma}^{0} p(\theta)\left(x(t-\tau+\theta) - x(t+\theta)\right) d\theta,$$

where

$$k_1 = \frac{3}{4} c_1 w h_0^{-1/4} = \left[\frac{\delta F_x}{\delta h} \right]_{h_0} ,$$

$p(\theta)$ is the force distribution on tool flank, τ is the time delay, and σ is the time for the chip to slide along the active face of the tool flank [20]. The length of the delay τ is equal to the time difference between two successive cuts which is the same as the time period of revolution in case of turning. Substituting this expression for force as a function of Δh in the equation of motion of the knife, we obtain:

$$\ddot{x} + 2\xi\omega_n \dot{x} + \omega_n x = \frac{\Delta F_x}{m} = \frac{k_1}{m}\left(\int_{-\sigma-\tau}^{-\tau} p(\tau+\theta)\, x(t+\theta)\, d\theta - \int_{-\sigma}^{0} p(\theta)\, x(t+\theta)\, d\theta \right).$$

Usui et al.[21] analytically derived that the shear stress distribution on the tool flank can be approximated by an exponential function of time and this was used by Stepan. Therefore, $p(\theta)$ can be approximated as

$$p(\theta) = \frac{1}{\sigma_0} e^{\frac{\theta}{\sigma_0}} \quad \text{where } \theta \in (-\infty, 0).$$

Using this expression for shear distribution in the equation of motion for the knife, and differentiating again with respect to time, we get the following:

$$\dddot{x}(t) + (1 + 2\xi\omega_n\sigma_0)\ddot{x}(t) + (2\xi\omega_n + \omega_{n^2}\sigma_0)\dot{x}(t) + \left(\omega_{n^2} + \frac{k_1}{m}\right)x(t) - \frac{k_1}{m}x(t-\tau) = 0$$

By assuming that the force on the tool flank is concentrated, which is justified if the active face is small as in the case of KESM, the time taken by the chip to slide over the active face of the tool flank (σ) is taken to be zero. With the inclusion of this, the above expression becomes

$$\ddot{x}(t) + 2\xi\omega_n \dot{x}(t) + \left(\omega_{n^2} + \frac{k_1}{m}\right) x(t) - \frac{k_1}{m} x(t-\tau) = 0.$$

This is a simplified model of cutting process with regenerative effects incorporated as the delay in the delay differential equation model. Stability analysis of this system is presented in Stepan [20] and the optimal cutting parameters can be chosen to fall within the stable boundaries of the stability chart. Using stability analysis [22][23], by substituting $x(t)=Ae^{(\lambda t)}$ where A and λ are complex numbers, we get the characteristic equation as

$$D(\lambda) = \lambda^2 + 2\xi\omega_n\lambda + \omega_n^2 + \frac{k_1}{m_1} - \frac{k_1}{m_1} e^{-\lambda\tau} .$$

Stability analysis of this system in terms of cutting speed and natural frequency gives us the stable domains of the cutting process.

H. Chatter model for KESM

Chatter in the sectioning process of KESM can be mainly attributed to the regenerative effect. This has been supported by the evidence from the measurement of the surface profile of both the section and the workpiece after cutting and the variation in acceleration of the diamond knife of KESM (see Chapter IV and Chapter V). Moreover, varying the cutting speeds across successive sections reduced the chatter in the image data and the chatter artifacts are aligned across those sections with a shift of phase. Hence, a major contribution to the chatter in the sectioning process of KESM comes from the regenerative effect of the uneven workpiece surface and the vibrations in the diamond knife feeding each other. This effect can be modeled as continuous sectioning of an uneven surface with a vibrating knife. Delay differential equations capture this kind of

system mathematically. The time delay in the DDE is due to the fact that any change in the acceleration of the knife is induced by the variation in the thickness of the section it is cutting, which itself is a result of the vibrations in the knife in the previous cut. Hence the acceleration of the knife acts on itself after a time delay and so is the chip thickness.

To model the chatter in the sectioning process of the KESM, we start with the universal oscillator model:

$$\ddot{x} + 2\xi\omega_n \dot{x} + x = 0 .$$

Since, we have a driven force due to the resistance offered by the workpiece material, we add this force to the above equation. For a simple model, we take the material resistance as proportional to the thickness of the chip that is being sectioned. To make the model one-dimensional, we assume that the rake angle and the friction angle remain constant over the sectioning process. This means that the force acting on the knife in the horizontal and the vertical directions are proportional to each other and the variation of the force in the horizontal direction is captured in the variation of the force in the vertical direction. Also, note that the thickness of the chip is equal to the difference between the current position of the knife (x(t)) and the position of the surface directly above the edge of the knife, which is the position of the knife in the sectioning stroke before this ($x(t-\tau)$). By substituting these, we obtain the equation for the knife position variation as:

$$\ddot{x} + 2\xi\omega_n \dot{x} + x = F_x = k\left(x(t) - x(t-\tau)\right), \text{ where k is a constant.}$$

Fig. 33 shows the variation in the chip thickness in the sectioning process of KESM as a function of time using the above model by substituting 0.2 for ξ, 100 for k and 120 for ω_n. The values for ξ and the proportionality constant k are chosen at random. Note that the simulation result from this model closely resembles the variation in acceleration of the

diamond knife of KESM measured during tissue sectioning (Fig. 22 and Fig. 23 in Chapter V). Moreover, intricate details such as the thickness remaining constant for the first half-a-second is captured by the model as can be seen in Fig. 33. It has also been observed that the imaging data for the first few sections cut in the KESM have little or no chatter artifacts.

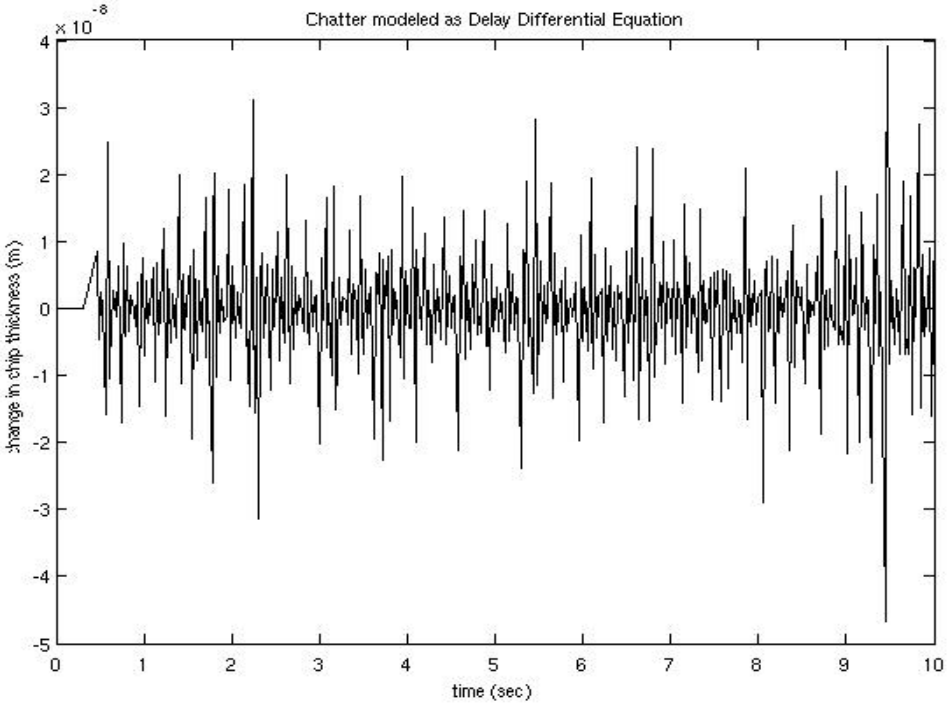

Fig. 33. Chatter observed as the variation in the chip thickness in KESM sectioning process modeled as a Delay Differential Equation.

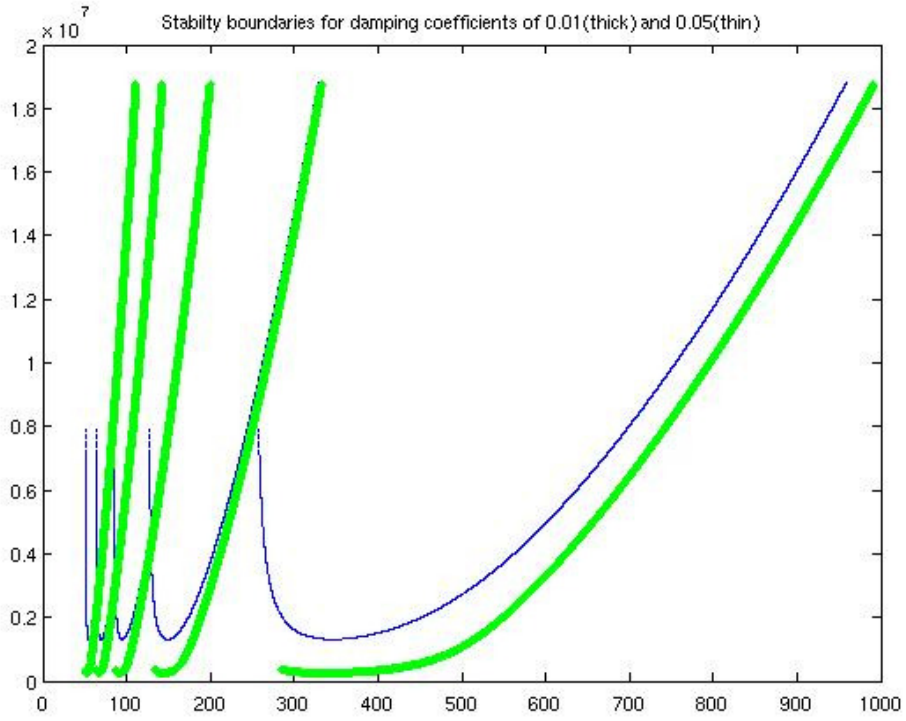

Fig. 34. Stable boundaries of the sectioning process as a function of M (a variable representing the cutting speed and is inversely proportional to it) and K(cutting coefficient) for damping coefficients of 0.01(thick) and 0.05(thin).

This model of the KESM sectioning process is mathematically similar to the model of the regenerative chatter proposed by Stepan. Hence, we can apply the stability analysis of Stepan's model to this model. Stability chart for this dynamic system provides the boundary between the stable and unstable domains. Fig. 34 shows the stability chart for the sectioning process model for KESM. It gives the stable boundaries for two different damping coefficients. Since the parameters (ξ and k) in this model are not experimentally determined, these stability charts do not give the sectioning speed range to be used for a give section thickness. But by comparing between different parameters, such as the damping coefficient, we can obtain the effects of different embedding polymers on the sectioning process stability.

I. Summary

Orthogonal metal cutting process provides a simple model of the sectioning process of the KESM. By identifying the forces involved in the system, this simple process can be modeled to capture the generation of nonlinearities in the sectioning process such as chatter. Some basic models of such a system are proposed in the metal cutting literature. Chatter, which can be fed by multiple sources, makes these models complex and difficult to study. Stepan's model gets rid of these difficulties by assuming that the nonlinearities in the cutting force as the only cause of nonlinearities in the sectioning process and subsequently modeling the process as a system of delay differential equations. It also makes the study of stability of the system possible. Hence, the sectioning process of the KESM is modeled using DDEs. Simulations of the model are shown to match closely with the observed chip thickness variation and the variation of the acceleration of the diamond knife during the sectioning process of KESM. Even though a few variables are assumed at random, stability charts from these model can still be used to compare different materials for embedding the tissue. Stability analysis using a more complete model can therefore be used to choose appropriate parameters of the sectioning process to abate chatter and to achieve a high quality volumetric imaging data.

CHAPTER VIII

IMAGE PROCESSING TO REMOVE CHATTER ARTIFACTS IN VOLUMETRIC DATASETS

A. Introduction

Knife chatter in KESM appears as optical artifacts in its volumetric image data sets. Abatement of chatter in the sectioning process normally requires a redesign of the process parameters such as speed of cutting, depth of cut, choice of polymer, etc. Though these changes may reduce subsequent chatter, changing the sectioning parameters is not always possible due to temporal resolution of the camera sensors and the limitations of the stage controller. Therefore, there is a grave need to remove chatter artifacts in the existing imaging data. This chapter presents appropriate image processing techniques to remove such artifacts from the data.

B. Knife chatter in image data

Chatter is a mechanical process characterized by an undesired relative vibration between the cutting tool and workpiece. These undesired vibrations leave their mark in image data, for instance from KESM. Relative vibration between knife and workpiece leads to uneven chip thickness, which is the main effect of chatter in metal cutting and has been well studied. In KESM, the tissue is concurrently imaged while cutting. Light for illuminating the tissue comes through the diamond knife and passes through the tissue

before it reaches the objective (Fig. 35). Waviness of tissue induced by these vibrations will therefore show up as variations in the intensity in the image. Chatter also can show up on imaging data from other microscopy techniques where the tissue is back-illuminated. In KESM, tissue sections are imaged while cutting and therefore vibration of the knife is also reflected in the image data as variation in focus.

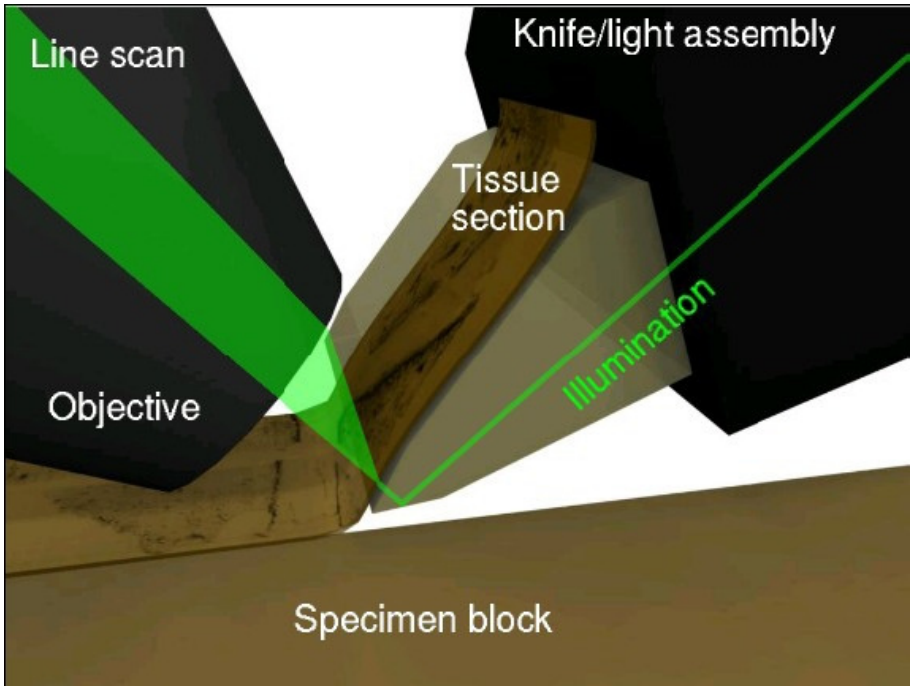

Fig. 35. Illumination of tissue for imaging in KESM [10].

C. Image processing techniques to remove chatter artifacts

Chatter is not entirely a random process. It appears at regular intervals on the surface of the chip. Fig. 5 shows the chatter as it appears in the image of a tissue section. The dark horizontal streaks due to chatter are more or less at a regular interval and are regularly repeated along the Y-axis. These regular patterns of chatter can be used to remove chatter artifacts from the imaging data. Two main effects of knife vibration on

image formation are light intensity variation and focus variation. These effects can be selectively reversed by increasing the intensity of the chatter lines and sharpening the region of chatter streaks.

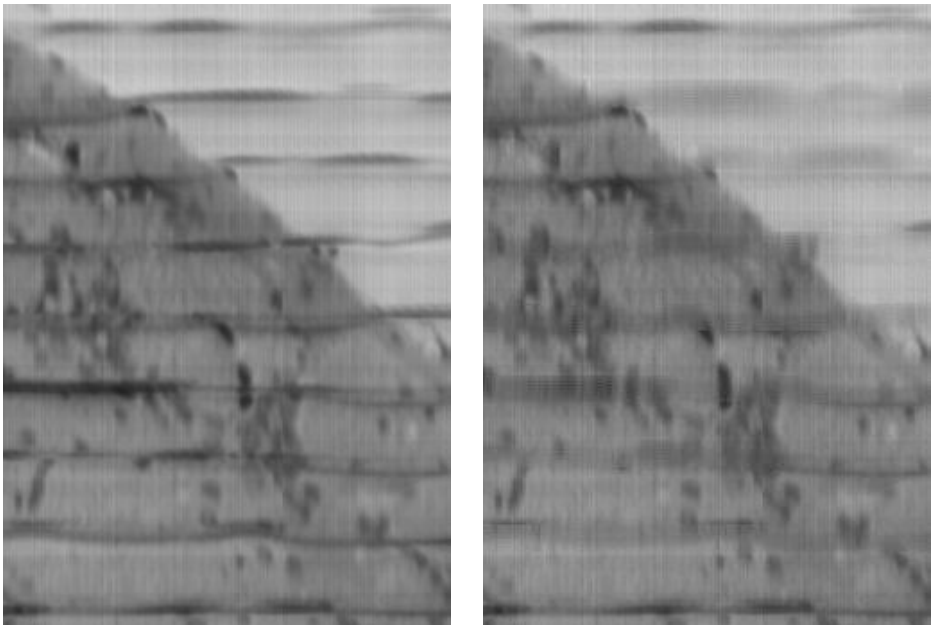

Fig. 36. Sectioned image from KESM with chatter (left) along with the processed image (right) by selectively smoothing the intensity.

Fourier transformation of the image data gives its frequency spectrum. Fig. 37 shows the Fourier transform of a tissue section image from KESM shown in Fig. 36. From this Fourier image it is evident that the image has high amplitude frequency components parallel to the Y-direction. These appear as chatter artifacts in the image. Frequency filtering the Fourier image, by truncating the high frequency components, leaves only frequencies that correspond to chatter streaks. By taking the inverse Fourier transform of this frequency-filtered Fourier image, we obtain the image with chatter artifacts singled out. Fig. 38 shows the original image with its frequency filtered image. This information can therefore be used to selectively process the image automatically at

required places (Fig. 36).

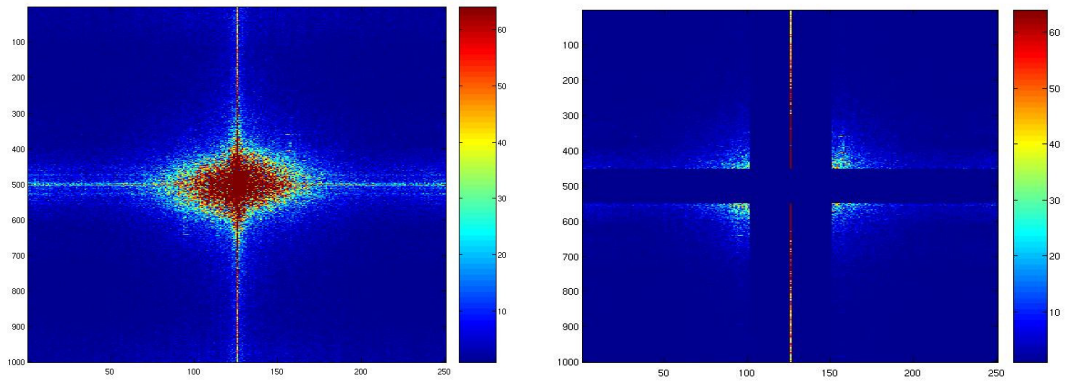

Fig. 37. Fourier image of the original image (left) and the filtered Fourier image to extract chatter artifacts (right).

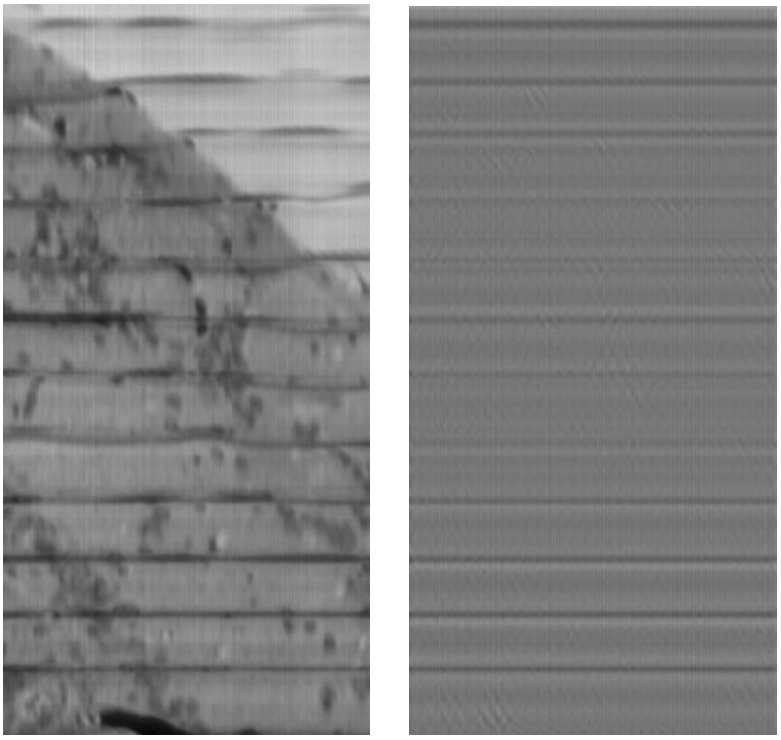

Fig. 38. KESM image data with chatter (left) and frequency filtered image using FFT (right).

Clearly the frequencies that appear on the Y-axis of the Fourier image alone gave

rise to the chatter artifacts. This information can be used directly to remove the artifacts.

D. Summary

Chatter in the sectioning process exhibits repeating patterns in the volumetric image data. This characteristic of the chatter can therefore be exploited to find and remove chatter artifacts. Knife chatter in the KESM results in uneven brightness and out-of-focus regions in the image data. Chatter artifacts can be removed by selectively reversing these effects in the data using frequency-dependent image processing. Spectral analysis of the image gives the necessary information about chatter location used in chatter removal.

CHAPTER IX

FREE-FORM NANOMACHINING FOR CHATTER ABATEMENT

A. Introduction

The KESM can currently section and image tissues down to 500nm thin. This section thinness is sufficient to reconstruct vascular structure and the sparse connectivity of neurons. In order to identify structures, such as synaptic vesicles (~35nm) and axonal and astro-glial processes of narrow diameter (~50nm dia.), the depth resolution of the KESM instrument needs to be improved by an order of magnitude. Many factors limit achieving such resolution, even though the vertical (lift) stage of KESM has an intrinsic resolution of 25nm in the Z-axis. Knife chatter remains the foremost limitations for achieving better Z-axis resolution in the KESM. As shown in Fig. 13 in Chapter IV, the observed variation in tissue section thickness can be hundreds of nanometers and therefore the desired section thickness of 50nm can never be achieved with this degree of chatter in the sectioning process. What is needed is a higher precision machining process that can actively control workpiece surface finish and chip (section) thickness while sectioning. In this chapter we examine the potential for chatter-free nanomachining using one such instrument, the ultra-precision diamond-turning lathe, as manufactured by Moore Nanotechnology Systems of Keene, New Hampshire, USA [24].

B. Advantages of using a lathe

Volumetric data resolution of the biological sectioning using KESM-like sectioning process, where the workpiece-cutting tool contact is intermittent, is drastically

limited by the undesired vibrations creeping into the sectioning process. Every time the workpiece and the cutting tool collide, the impact of the contact initiates oscillations in the diamond cutting tool. Fig. 23 in Chapter V shows this effect of impact on the acceleration of the diamond knife of the KESM. By maintaining continuous contact between the workpiece and the cutting tool, these undesirably impacts are avoided. Face cutting using a lathe is therefore suggested as an alternative to attain impact-free sectioning. Since ultra-precision and ultra-stable diamond-cutting lathes are commercially available [24], they are examined below as potential candidates to achieve stable, chatter-free, physical sectioning for high-resolution biological 3D microscopy.

C. Free-form nanomachining

Though ultra-precision machining technology started three decades ago, it was expensive and was specialized for certain jobs. In recent years major advancements in controls, feedback systems, servo drives, and general machine design and construction have opened ultra-precision machining to a wider variety of applications, particularly in the photonics industry, by making nanomachining more productive, precise, and less expensive. Current single point diamond turning lathes utilizing these new technologies allow surfaces to be machined into a surface tolerance as low as 2nm root mean square error. This precision is achieved due to various incremental improvements in machining, such as using [24]:

- granite machine bases, for thermal and mechanical stability, damping characteristics, lower center of mass, and design flexibility,
- hydrostatic oil bearing box-way linear axes, for enhanced damping, smoothness of motion, geometrical accuracy, and wear-free operation,

- high-speed air bearing spindles allow faster feed rates, therefore reduced cycle times, as well as smooth rotational motion, high load capacity, and stiffness,
- high speed CNC (computer numerical control) controls to allow networking, massive part program storage, and use of advanced drive and feedback devices to improve workpiece accuracy,
- high-resolution linear scales, providing precise axis position feedback for nano-metric incremental moves, improved dimensional stability, and consistent and precise geometrical accuracy, and
- on-machine workpiece measurement and error compensation systems allow residual workpiece errors to be assessed, and practically eliminated, providing they are of a repeatable nature.

A current state-of-the-art single point diamond-turning lathe is shown in Fig. 39. This machine has the spindle mounted on the X-axis, and for face cutting would typically have the diamond turning tool mounted along the Z-axis. The axes are mounted in a "T" configuration, and as such allow any rotationally symmetrical part to be machined. Fig. 40 shows how the vertical Y-axis is buried within the Z-axis, rather than stacked one stage above the other. The machine base comprises a massive granite slab adding extra stability to the machine. An advanced CNC controller with PC front end is utilized, while 10nm linear scales provide position feedback. Many advanced design features are built in these machines such as integral axis configuration, to improve system stiffness, reduce thermal effects, and reduce geometrical errors. Advanced PC-based CNC motion controllers are now used in conjunction with athermalized linear scale feedback devices and previously illustrated state-of-the-art linear motors, allowing surfaces as smooth as 2nm to be generated directly from the machine.

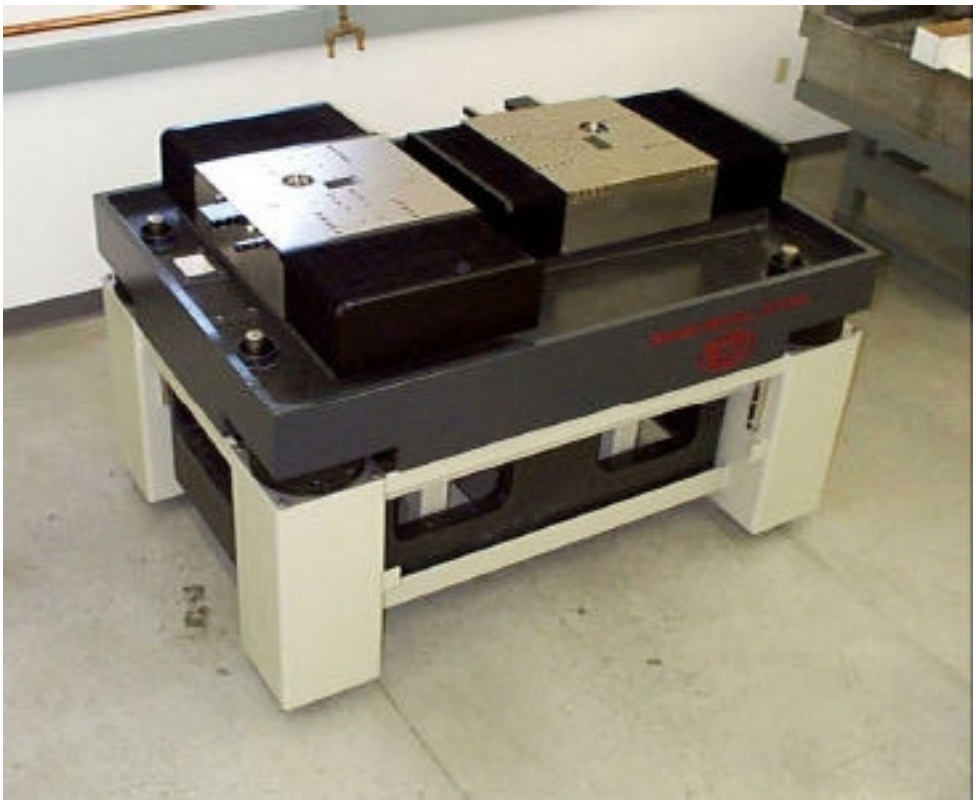

Fig. 39. Free form nanomachine showing the base and T-configuration of the stages [24].

D. Slow slide servo

A new breed of such multi-axis machines has been developed that are able to generate shapes not limited to rotational symmetry, but extending to free-form geometries. Slow slide servo is a novel machining process capable of generating free-form optical surfaces or rotationally asymmetric surfaces at high levels of accuracy. In able to achieve good results with this technology some key parameters need to be satisfied. These parameters include tool path generation, tool radius correction, machine set-up, servo system performance, and the CNC computing capabilities.

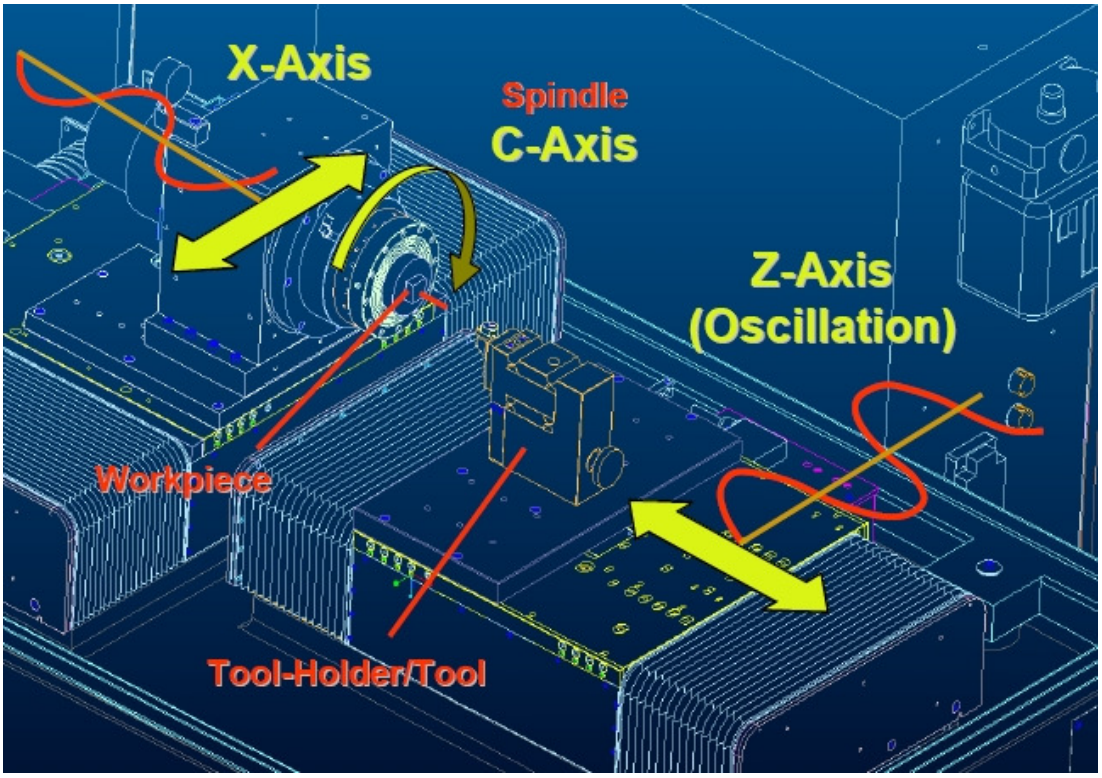

Fig. 40. Moore Nanotechnology 350UPL, a commercially available free-form nanomachine, showing co-ordinate system [8].

A typical diamond turning lathe consists of two linear axes and a spindle, or rotary, axis (Fig. 40). Both linear axes, X and Z, are position controlled. The rotary axis is velocity controlled but can also be position controlled by adding an optical encoder. In this technique, the Z-position is a function of both X-axis and the work spindle position or C-axis position. The diamond tool is mounted along the Z-axis of a lathe and the part with the free-form surface or non-symmetric surface is mounted on the work spindle. As the part rotates, the Z-axis carrying the diamond tool oscillates in and out in a sine wave type motion to generate the surface. Depending on the amplitude of the sine wave, frequencies up to 60 Hz can be obtained. The C-axis rotates the work piece about the Z-axis, and is position controlled to very high accuracy. The position loop bandwidth of the C-axis, which is a measure of system performance, is typically above 120Hz.

E. Moore Nanotechnology 250UPL ulra-precision diamond-turning lathe

The Moore Nanotechnology 250UPL is a commercially available ultra-precision free-form nanomachines. This is a diamond turning lathe with "T" shape configuration with the spindle mounted on the X-axis and the diamond tool on the Z-axis. The spindle can operate in two different modes, velocity mode or position mode. The spindle is used in velocity mode for typical axis-symmetric diamond turning work with a maximum speed of 10,000 RPM. In the position mode the spindle uses an optical encoder to close the angular position loop. The same actuator motor and amplifier is used for both configurations. The feedback resolution of all the three axes is 0.034nm and the positioning accuracy of the rotational axis is +/- 2 arc-seconds [24]. These specifications make it an ideal free-form nanomachine that can be adapted to use for physical sectioning in biology.

F. High-resolution physical sectioning for biological 3D microscopy

Sectioning of biological tissue for high-resolution volumetric imaging can exploit the above mentioned techniques of ultra-precision free-form nanomachining. Commercially available nanomachines have achieved accuracy levels of 2nm with hard materials like metals and glass, which makes these machines promising candidates to observe structures like synaptic vesicles and thin diameter axons.

Face cutting using an ultra-precision lathe has been proposed as a method of achieving chatter-free sectioning [25] as it eliminates repeated impact of the workpiece on the cutting tool. A cutting step in facing involves sectioning a ring on the end face of the cylindrical workpiece. Hence, the geometry of tissue sections obtain by using this process differs from those obtained by using a linear sectioning ultra-microtome or a

KESM employing linear stages. Also, the workpiece used in the lathe should be rotationally symmetric (a cylinder for example). Tissue samples can be embedded in the cylindrical workpiece in an axially symmetric manner, as shown in the Fig. 41.

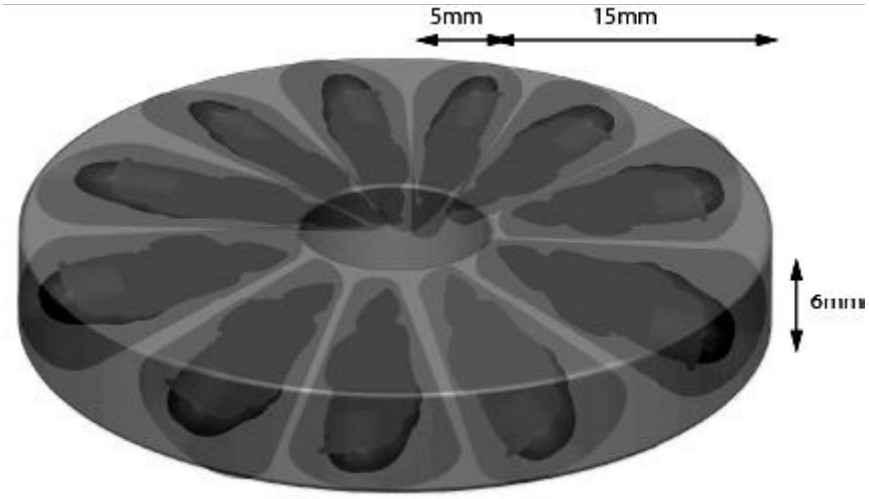

Fig. 41. Tissue samples embedded in an axially symmetric manner in the workpiece for facing process using an ultra-precision lathe (illustration prepared by Wonryull Koh) [25].

G. Issues in using the lathe for high-resolution physical sectioning

The 2nm accuracy levels in the surface machining achieved by the commercially available machines are attained cutting hard materials such as glass and metals. Therefore, there is no assurance that a comparable level of tolerance can be attained cutting a workpiece made of polymer. (Though during sectioning, the knife may be held vibration-free, there is still the possibility that the polymer performs wave-like deformations in front of the knife.) Though sectioning ultra-thin tissue sections is possible with these machines, they have never been applied to also provide concurrent imaging as in the KESM. Typically, the workpiece surface has been critically examined, but never has the focus been on the quality of the chip, or section. One readily available alternative to avoid concurrent imaging altogether is to collect the sections and preserve

them to be imaged later as done in techniques like Array Tomography and ATLUM. If concurrent imaging is to be employed, compensation must be made for the cylindrical geometry of the workpiece. Sampling intervals of the line scan camera at the outer edge and the inner edge of the workpiece must be approximately equal. This can be resolved by adjusting the line scanning rates of the camera based on the distance from the axis of the workpiece. Clear plastic between embedded specimens can be skipped over by inhibiting line sampling for these clear patches.

H. Chatter abatement using free-form machining

Chatter in the sectioning process can also be abated by using the free-form machining technique. Primarily, chatter leaves its mark in the form of a wavy surface on the workpiece and alternating bright and dark bands on the imaging data. This unevenness of surface profile feeds the chatter in the next cut. These chatter artifacts, and therefore the variation in the surface profile, vary continuously across successive sections, as shown in Fig. 6 in Chapter III. The alternating chatter bands retain the same frequency and continuously vary in phase across successive sections. This information can be used to predict the surface profile of the next section. Once the surface profile of the section to be cut has been predicted, the CNC program that controls the motion of the cutting tool can be altered to take this surface variation into account and modify its tool-path accordingly. The section that is generated using this modified path should be more uniform in thickness and hence exhibit less chatter. By actively suppressing chatter in the sectioning process, we can hope to achieve a chatter-free physical sectioning and high-resolution, high-quality volumetric data.

I. Summary

Advancements in machining can be applied to biological tissue sectioning to obtain high-resolution volumetric tissue data sets in less time. Using an ultra-precise lathe eliminates problems in current sectioning processes such as repetitive impact of the workpiece and the cutting tool due to their intermittent contact, and subsequent generation of the regenerative chatter. Going further, we suggest the use of *free-form nanomachining,* a novel technique of machining used to manufacture ultra-precise parts with free-form geometries. Adapting this technology to biological sectioning involves issues like achieving concurrent imaging and of course needs experimental verification... Free-form nanomachines are commercially available and Moore Nanotech 250UPL is presented as one promising alternative. The issues of embedding the tissue samples, achieving concurrent imaging, and obtaining high surface accuracy are presented with possible solutions to each. Resolving these issues of adapting optical imaging feedback into the free-form nanomachining repertoire may make acquisition of high-resolution volumetric tissue structure a reality.

CHAPTER X

ULTRATHIN SECTIONING USING AN OSCILLATING KNIFE

A. Introduction

Sectioning tissues down to the order of tens of nanometers at a reasonably fast rate is currently limited by instabilities in machining. The use of free-form nanomachining techniques overcomes this problem in machining. Although nanomachining has been proven to produce accurate surface profiles for hard materials like metals, machining polymers for ultrathin sections suffers from the problem of compression due to their softness/viscoelasticity. Compression of the polymer results in a thicker section and distorts the cellular structure. Oscillating knives overcome this problem of compression by reducing the sectioning angle. In this chapter we introduce sectioning using oscillating knives as a potential approach to obtain high quality ultrathin tissue sections and thereby high-resolution chatter-free volumetric data sets.

B. Ultrathin sectioning

So far, we have seen that the ultrathin sectioning for biological microscopy has been limited by stability of the sectioning process. Apart from this, polymers used for embedding the tissue samples, being viscoelastic, are also compressed under the force of the cutting tool. This results in thicker and shorter sections and also leads to frictional chatter [26]. In percentage, the compression of the section sectioned with a knife angle of 45 degrees is about 40% [27]. Cryo-sections of vitreous samples are even more

compressed (up to 60%) than the resin embedded samples [27]. This heavy compression implies that the ultrathin sections are twice as thick as expected. This becomes a major problem if the tissues are to be sectioned down to tens of nanometers in thickness. Compression also becomes a limiting factor in the electron topographic analysis of frozen-hydrated sections [28][29]. In addition to deteriorating the imaging resolution, it results in the distortion of the cellular structure. Thus, uncompressed ultrathin sections would mean a better tissue structural data of the tissue.

The amount of compression in polymers depends on various factors such as the angle of the knife, hardness of the polymer, and the section thickness. Therefore to obtain ultrathin sections of a given polymer, knife angle has to be carefully chosen. Jesior showed that using a smaller knife angle improves the structure of ultrathin sections by reducing the compression of the polymer [30] and the amount of compression was shown to be approximately equal to the knife angle [27]. Hence, reducing the knife angle reduces the compression thereby increasing the quality of the section and structure. On the contrary, using a smaller knife angle for sectioning brittle materials such as thermoset polymers (such as epoxy resins) leads to elastic fracture. Sectioning with a smaller knife angle results in crack formation at an oblique downward angle which results in a discontinuous and blocky chip. This process is called discontinuous-crack type chip formation [9]. This puts a limit on how small a knife angle can be. Also, small-angled knives have a lower cutting edge quality and a considerably shorter life span [9].

Oscillating knives provide an answer to these problems. Experiments indicate that the ultrathin sections produced with an oscillating diamond knife are almost uncompressed without exhibiting additional cutting artifacts [31]. Sectioning with an oscillating knife is also shown to suppress chatter [5].

C. Oscillating knife

Studer and Gnaegi invented the oscillating diamond knife to minimize the compression in ultrathin sectioning if the polymer [32]. Oscillating knife consists of a diamond knife with a piezoelectric oscillator mounted on it. Alternating voltages of desired frequency and amplitude are applied to the piezoelectric mount which then oscillates the knife along the cutting edge.

Oscillating the knife along the cutting edge makes the sectioning angle smaller than the angle of the knife. The same effect can be achieved by tilting the knife by an angle to the cutting direction. But tilting the stroke is known to cause problems in ultramicrotomy and results in poor quality sections due to the curling of the chip [32]. Oscillating the knife does not have this problem. While sectioning with an oscillating knife, since the volume of the section remains the same, the section becomes thinner at the same depth of cut due to increase in the length of the stroke.

Oscillating diamond knives for ultrathin polymer and biological sectioning at room temperature are commercially available from Diatome under the name of *ultra sonic.* An oscillating knife for low temperature application called oscillating cryo-knife is in development [26]. The ultra sonic knife produces ultra-thin sections almost free of compression, with biological samples embedded in Epon, Araldite, and acrylic resins (LR White) [33].

Diatome's ultra sonic knife is available with a wedge angle of 35 degrees and a cutting range of 10-100nm. The length of the knife is 3mm and the peizoelectric actuator can oscillate in the 20-45kHz frequency range [33].

D. Summary

High-resolution chatter-free volumetric tissue structure data requires ultrathin sectioning of the embedded tissue samples, which is currently limited by the instabilities in the sectioning process. Though, using free-form nanomachining techniques allow a stable sectioning of hard materials like metals, polymers, being soft and viscoelastic, suffer from compression of the section. Compression of the polymer during sectioning results in a structurally distorted thick section, and hence a low-resolution image data. Though the use of low-angle diamond knives has been shown to improve ultra-structural preservation of ultrathin sections, small angled knives produce cracks in the chip and also have a shorter life span. Oscillating knives overcome these problems by achieving a smaller sectioning angle without reducing the knife angle. Commercially available oscillating knives such as Diatome ultra sonic can achieve ultrathin compression-free biological sections. Hence, oscillating knives can be used in conjunction with the free-form nanomachining to obtain high resolution chatter-free volumetric tissue data sets.

CHAPTER XI

CONCLUSIONS AND FUTURE WORK

A. Summary and conclusions

In this thesis we have instigated the engineering study of the physical sectioning process for 3D biological microscopy. We have introduced various 3D microscopy techniques using physical sectioning and compared them (Table 1). Any technique using physical sectioning potentially suffers from the undesired vibrations in the sectioning process called chatter. Chatter limits the Z-axis resolution of the 3D microscopy and affects the quality of the reconstruction by introducing artifacts in the imaging data. To understand and subsequently abate this chatter, a systematic study of the sectioning process with special emphasis on chatter has been undertaken, first characterizing the process and then subsequently modeling it. Table 2 presents a brief overview of various characteristics of the sectioning process and the chatter along with the instruments that we used to measure those characteristics and the data obtained with concluding remarks.

Table 3. Characteristics of the sectioning process and the chatter.

S.no	Characteristic type	Recording Instruments/Tools	Data	Remarks
1.	Acoustic	Microphone	Sound of the sectioning process.	Frequency spectrum of sound from the sectioning process gives an estimate of the quality of the process and can be used to identify chatter.
2.	Geometric	Profilometer and Atomic Force Microscope	Surface profile of the tissue section and/or the workpiece.	Surface profile measurement of the tissue sections using a profilometer resulted in dragging and compression of the soft tissue. AFM measured the profile in a tapping mode and showed that the variation in the chip thickness due to chatter is significant.
3.	Optical	KESM, Fourier transform, and image processing tools.	Analysis of the image data recorded by KESM.	Fourier analysis of the image data of the KESM with chatter artifacts revealed chatter frequencies and suggested a way to extract or eliminate the chatter artifacts.
4.	Vibrational	Accelerometer.	Lateral acceleration of the diamond knife of the KESM during tissue sectioning.	Acceleration of the knife gives information on the forces acting on the system including those generated by the erratic chatter. Acceleration data corresponds to the artifacts in the image data.
5.	Polymer	Digital Durometer and Nanoindenter.	Hardness of the polymer material and the response of the thin films of these materials to an applied force.	Hardness of the embedding polymer can be quickly measured using a digital Durometer and can be compared with other polymers for high-quality sectioning. Nanoindenter provides more accurate response characteristics of the material as thin film but requires specimen preparation before measurements can be taken.

The main results of our analysis of the measurements obtained for the characterization of the chatter can be summarized as follows:

1. Surface profile measurements of the sections from the KESM showed that the section thickness varied as much as the desired chip thickness.
2. Comparison of the surface profile of sections cut at different cutting speeds and thicknesses revealed that:
    a. the frequency of the chatter (measured as variation in chip thickness) increases as the desired section thickness increases,
    b. the variation in the surface profile, which represents the variation in chip thickness, increases as the desired section thickness increases,
    c. the variation in the surface profile decreases as the sectioning speed increases.
3. Frequency analysis of the chatter artifacts in the imaging data support the conclusions obtained from the surface profile analysis.
4. Frequency analysis of the variations in the surface profile and the chatter artifacts in the imaging data match up giving an indication that the imaging artifacts are due to the distortions in the section geometry.
5. Fourier analysis of the knife acceleration data recorded during sectioning in the KESM and that of the chatter artifacts in the corresponding imaging data revealed that the predominant frequency in these data sets is the same, concluding that the vibrations of the knife correspond to the imaging artifacts.

Based on the analysis of the data obtained from these measurements, and by matching the chatter characteristics from different sources like the artifacts in the imaging data, surface profile of the tissue sections, and the variation in the knife acceleration, we concluded that regenerative chatter is the predominant chatter mechanism in the

sectioning process of the KESM.

We introduced some important nonlinear dynamical models, drawn from the metal machining literature, of the sectioning process that account for chatter. Modeling the sectioning process of the KESM and subsequent comparison of the model with the observed data is summarized below:

1. The sectioning process in the KESM with regenerative chatter was modeled as repeated planing of the uneven workpiece surface. This has been mathematically captured in a delay differential equation.
2. The frequency of the variation in the chip thickness obtained from this model was found to be comparable to the surface profile data obtained from the measurements.
3. The model also indicates that the initial sections do not suffer from the chatter which has been observed in the KESM sectioning process and matches with the the imaging data obtained for the first few sections.
4. Comparison of embedding polymers with different hardness values emulated as different damping coefficients in the model, matches with the observation from the analysis of the knife acceleration data that the chatter dampens out on the softer material (soft brain tissue, as opposed to hard plastic).

Although the model lacks some parameters, stability analysis of this system provides the comparison between different embedding polymers for stable sectioning. For the volumetric data that have previously been acquired with chatter artifacts, we presented image processing techniques as methods abating these chatters artifacts. Finally, we introduced ultra-precise machining techniques, using (1) free-form nanomachining and (2) an oscillating knife, as potential ways to acquire chatter-free higher-resolution

volumetric data.

B. Future work

Future developments to improve both the physical sectioning and imaging processes are needed as the demand for higher resolution volumetric tissue data has grown. Most notably, adapting the ultra-precise machining techniques to biological sectioning and using an oscillating knife to acquire high-resolution volumetric data could potentially open up a faster and easier way to obtain 3D tissue structure data and thereby aid in the accurate modeling of the biological processes. The issue of achieving high surface accuracy using soft polymer embedding materials has yet to be resolved to make complete use of ultra-precise free-form nanomachining. An alternative approach is *cryo-sectioning*, wherein the hard vitrified tissue sample is directly sectioned, bypassing the polymer embedding altogether [34][35]. Another added advantage of this later technique is that subcellular processes in those tissue sections can be rejuvenated to life [36]. Techniques to preserve intact the inter-cellular signaling during the vitrification phase and preservation phase would be of a great scientific importance and demand a systematic study.

Merging various 3D biological microscopy techniques using physical sectioning, such as KESM and Array Tomography, is another promising approach and also needs serious study. Such instrument mergers help in concurrently acquiring volumetric data of the tissue samples at multiple-scales, and thereby could provide better understanding of the biological mechanisms in those tissues. Table 3 gives the possible mergers between various techniques using physical sectioning for 3D biological microscopy.

Table 4. Possibility of merger between various physical sectioning techniques.

Technique	**KESM**	**Array Tomography**	**ATLUM**
Array Tomography	X		
ATLUM	X		
Serial section TEM		X	X
SBFSEM		X	

The merger between the KESM and the ATLUM seems the most promising as both techniques use an automated sectioning process. KESM images the tissue during the sectioning and the tissue chips could be preserved in a ribbon, as is done in the ATLUM for later imaging with SEM or TEM. This demands a serious study as it provide both light microscopy and electron microscopy data of the tissue sample at different resolution scales. Similarly, the techniques of KESM and the Array Tomography can be merged, if the tissue sections in the former can be collected and preserved for use with Array Tomography. Array Tomography and serial section TEM also go together as the array of the tissue sections obtained in the former can later be imaged in a TEM to obtain a serial section TEM data. Study of the possibility of these mergers can result in data acquisition at multiple resolutions, and thereby speed up multi-scale modeling of the biological processes based on the collected volumetric tissue data.

REFERENCES

[1] D. L. Spector and R. D. Goldman, *Basic Methods in Microscopy: Protocols and Concepts from Cells, a Laboratory Manual,* Cold Spring Harbor Laboratory Press, Cold Spring Harbor, NY, 2005.

[2] D. M. Mayerich, *Acquisition and Reconstruction of Brain Tissue Using Knife-Edge Scanning Microscope.* M.S. Thesis, Dept of Computer Science, Texas A&M University, 2003.

[3] K. J. Hayworth, N. Kasthuri, R. Schaleck, and J. W. Lichtman, "Automating the Collection of Ultrathin Serial Sections for Large Volume TEM Reconstructions," *Microscopy and Microanalysis*, vol. 12, Suppl. 2, pp. 86-87, August 2006.

[4] K. Micheva and S. J. Smith, "Array Tomography: A New Tool for Imaging the Molecular Architecture and Ultrastructure of Neural Circuits," *Neuron*, vol. 55, no. 1, pp. 25-36, 2007.

[5] W. Denk and H. Horstmann, "Serial Block-Face Scanning Electron Microscopy to Reconstruct Three-Dimensional Tissue Nanostructure," *PLoS Biology*, vol. 2, no. 11, pp. 1900-1909, 2004.

[6] K. M. Harris, E. Perry, J. Bourne, M. Feinberg, L. Ostroff, and J. Hurlburt, "Uniform Serial Sectioning for Transmission Electron Microscopy," *J. Neuroscience*, vol. 26, pp. 12101-12103, 2006.

[7] M. Wiercigroch and E. Budak, "Sources of Nonlinearities, Chatter Generation and Suppression in Metal Cutting," *Phil. Trans. R. Soc. Lond. A.*, vol. 359, pp. 663-693, 2001.

[8] Y.E. Tohme and J.A. Lowe, *Machining of Freeform Optical Surfaces by Slow Slide Servo Method*, Moore Nanotechnology Systems LLC, PPT presentation, 2004.

[9] A. Kobayashi, *Machining of Plastics*, McGraw-Hill, New York, 1996.

[10] D. Mayerich, B. H. McCormick, and J. Keyser, "Noise and Artifact Removal in Knife-Edge Scanning Microscopy," in *Proceedings of IEEE International Symposium on Biomedical Imaging,* pp. 556-559, 2007.

[11] Material Characterization Facility, http://www.chem.tamu.edu/cims/Cleanroom.html (accessed on 10/01/2007).

[12] G. Binnig, C. F. Quate, and C. Gerber, "Atomic Force Microscopy," *Phys. Rev. Lett.*, vol. 56, no. 9, pp. 930-933, 1986.

[13] Veeco, http://www.veeco.com/products/details.php?cat=1&sub=1&pid=177 (accessed on 10/01/2007).

[14] PCB Piezotronics, http://www.pcb.com/spec_sheet.asp?model=352A24&item_id=10021 (accessed on 10/01/2007).

[15] E. Oberg, F. D. Jones, H. L. Horton, H. H. Ryffel, C. J. McCauley, R. M. Heald, M. I. Hussain, *Machinery's Handbook*, Industrial Press, New York, 2004.

[16] Y. C. Fung and P. Tong, *Classical and Computational Solid Mechanics,* World Scientific Publishing Company, Singapore, 2001.

[17] Rex Gauge Company, Inc., https://rexgauge.securesites.net/models.php?category=Digital%20DD-3

(accessed on 10/01/2007).

[18] Hysitron Incorporated, http://www.hysitron.com/Products/ProductPages/products_triboindenter.htm (accessed on 10/01/2007).

[19] M. E. Merchant, Mechanics of Metal Cutting Process, *J. App. Phys.*, vol. 16, pp. 267-275, 1945.

[20] M. Wiercigroch and A. M. Krivstov, "Frictional Chatter in Orthogonal Metal Cutting," *Phil. Trans. R. Soc. Lond. A.*, vol. 359, pp. 713-738, 2001.

[21] G. Stepan, "Modelling Nonlinear Regenerative Effects in Metal Cutting," *Phil. Trans. R. Soc. Lond. A.*, vol. 359, pp. 739-757, 2001.

[22] E. Usui, T. Shirakashi, and T. Kitagawag, "Analytical Prediction of Three Dimensional Cutting Process," *J. Engng. Industry*, vol. 100, pp. 236-243, 1978.

[23] S. H. Strogatz, *Nonlinear Dynamics and Chaos: With Applications in Physics, Biology, Chemistry, and Engineering*, Addison Wesley Publishing Company, Boston, 1994.

[24] Moore Nanotechnology Systems,. http://www.nanotechsys.com/NanotechProducts.html (accessed on 10/01/2007).

[25] B. H. McCormick, M. Wiercigroch, and D. Mayerich, *Knife-Edge Scanning Microscope Using an Ultra-Precision 3-Axis CNC Diamond Turning Lathe*, Technical Report, Department of Computer Science, Texas A&M University, College Station, TX, May 2005.

[26] A. Al-Amoudi, J. Dubochet, H. Gnaegi, W. Luthi, and D. Studer, "An Oscillating

Cryo-knife Reduces Cutting-induced Deformation of Vitreous Ultrathin Sections," *Journal of Microscopy*, vol. 212, pp. 26-33, 2003.

[27] K. Richter, "Cutting Artifacts on Ultrathin Cryosections of Biological Bulk Specimens," *Micron*, vol. 25, no. 4, pp. 297-308, 1994.

[28] C.E. Hsieh, M. Marko, J. Frank, and C.A. Mannella, "Electron Tomographic Analysis of Frozen-hydrated Tissue Sections," *Journal of Structural Biology,* vol. 138, pp. 63-73, 2002.

[29] J.R. McIntosh, "Electron Microscopy of Cells: A New Beginning of a New Century," *The Journal of Cell Biology*, vol. 153, pp. 25-32, 2001.

[30] J. C. Jesior, "Use of Low-angle Diamond Knives Leads to Improved Ultrastructural Preservation Ultrathin Sections," *Scanning Microscopy Supplement,* vol. 3, pp. 147-52, 1989.

[31] J.S. Vastenhout, J.D. Harris, "Improved Sectioning of Polymers Using an Oscillating Diamond Knife for Transmission Electron Microscopy," *Microscopy Today*, vol. 14, no. 5, pp. 20-21, 2006.

[32] D. Studer, H. Gnaegi, "Minimal Compression of Ultrathin Sections with Use of an Oscillating Diamond Knife," *Journal of Microscopy*, vol. 197, no. 1, pp. 94-100, 2000.

[33] Diatome, http://www.diatome.ch/en/products/pdf/ultrasonic_flyer_ENG_0907.pdf (accessed on 10/01/2007).

[34] J. Lemler, S. B. Harris, C. Platt, T. M. Huffman, "The Arrest of Biological Time as a Bridge to Engineered Negligible Senescence," *Annals of the New York*

Academy of Sciences, vol. 1019, pp. 559-563, 2004.

[35] G.M. Fahy, B. Wowk, J. Wu, J. Phan, and C. Rasch, "Cryopreservation of Organs by Vitrification: Perspectives and Advances," *Cryobiology*, vol. 48, pp. 157-178, Apr. 2004.

[36] G.M. Fahy, B. Wowk, J. Wu, "Cryopreservation of Complex Systems: The Missing Link in the Regenerative Medicine Supply Chain," *Rejuvenation Research*, vol. 9, no. 2, pp. 279-291, 2006.

VITA

Jyothi Swaroop Guntupalli graduated from the Indian Institute of Technology Madras (IIT Madras), Chennai, India, in 2005 with a B.Tech. in mechanical engineering. He enrolled at Texas A&M University in 2005 to pursue graduate study in computer science.

He can be contacted by email at swaroopgj@gmail.com.